DOI: 10.1002/ejic.201000525

# Ferrocene-Containing Coordination Polymers: Ligand Design and Assembled Structures

**Ryo Horikoshi[a] and Tomoyuki Mochida*[b]**

**Keywords:** Iron / Metallocenes / Metallacycles / Crystal engineering / Self-assembly

This review describes the preparation and structures of ferrocene-containing coordination polymers with a focus on ligand design. Neutral ligands such as heteroaryl ferrocenes and anionic ligands such as ferrocenyl carboxylates can be used to construct one-dimensional coordination polymers of various structural types. The main-chain and side-chain polymer structures are designed, and the conformational flexibility of ferrocenes leads to structural variety. The use of additional bridging ligands along with the anionic ligands leads to extended one- to three-dimensional structures. These complexes exhibit various properties, including characteristic redox activities.

## Introduction

In the last decade, the design and construction of coordination polymers has become an increasingly important area of coordination chemistry.[1] Coordination polymers can be obtained by the reaction of metal salts with bridging ligands, usually in high yields, and their guest-inclusion and magnetic properties, as well as their structural variety, have drawn particular interest. Ferrocene-containing coordination polymers can be constructed by using ferrocene-based ligands. The structural variety of these polymers originates from flexible ligand design as well as the conformational flexibility of ferrocenes. Ferrocenes are well known for their synthetic diversity, redox and magnetic properties, and other features.[2] The cyclopentadienyl (Cp) rings of ferrocene can be easily functionalized,[3a] and their properties can be controlled by the choice of substituents.

Even before the recent development of ferrocene-containing coordination polymers, ferrocene-containing polymers consisting of covalently linked ferrocenes had been studied extensively.[3] These polymers have drawn attention from synthetic chemists with regard to their possible applications.[2,3] The electrochemical properties of ferrocene-containing polymers are of particular interest. For example, polyferrocenyl compounds often exhibit a mixed-valent state, leading to changes in physical properties such as electrical conductivity.[3] Although these ferrocene-containing polymers are interesting, structural information on them is rather limited. In contrast to these pristine covalently linked polymers, ferrocene-containing coordination polymers form as brittle solids, a disadvantage for mechanical applications, and they do not maintain their structure in solution. However, their assembled structures can be designed, and their

[a] Department of Energy & Hydrocarbon Chemistry, Graduate School of Engineering, Kyoto University,
Kyoto-Daigaku Katsura,
Nishikyo-ku, Kyoto 615-8510, Japan
[b] Department of Chemistry, Graduate School of Science, Kobe University,
Rokkodai, Nada, Kobe, Hyogo 657-8501, Japan
E-mail: tmochida@platinum.kobe-u.ac.jp

*Dr. Ryo Horikoshi was born in Saitama, Japan, in 1972. He graduated from Toho University in 1997, and received his doctorate (science) from Toho University in 2002. After two years as a postdoctoral fellow at Kwansei Gakuin University and Ibaraki University, he worked in the petrochemical and automotive catalyst industries. He is currently on the technical staff of Kyoto University; his research interests are inorganic chemistry and chemical education.*

*Professor Tomoyuki Mochida was born in Kagoshima, Japan, in 1967 and graduated from the University of Tokyo in 1990. He joined the Institute for Molecular Science as a research associate in 1994 and received his PhD from the University of Tokyo in 1995. In 1997 he moved to Toho University as a lecturer, becoming an associate professor in 2003. From 1997 to 2000, he was engaged in a JST PREST (Precursory Research for Embryonic Science and Technology) project. He is currently a professor at Kobe University; his research interests are molecular magnets, ionic liquids, and proton transfer phenomena.*

  

periodic, stereoregular structures in the solid state are advantageous in terms of structural determination and electronic properties.[1]

Similar to conventional ferrocene-containing polymers, main-chain[4a] and side-chain[4b] structures of ferrocene-containing coordination polymers can be designed (Figure 1). The former contain ferrocenes in the polymer backbone, while the latter contain them as pendant ligands. Furthermore, high-dimensional coordination polymers can be formed by the introduction of an additional bridging ligand. Even the building units of the coordination polymers are isolated in some cases. For example, the reaction of ferrocene-containing ligands with metal ions sometimes affords discrete clusters, analogous to dimers or oligomers in polymer chemistry.[5] The design of assembled structures for ferrocene-containing coordination polymers is interesting from the viewpoint of supramolecules and crystal engineering.[1,2]

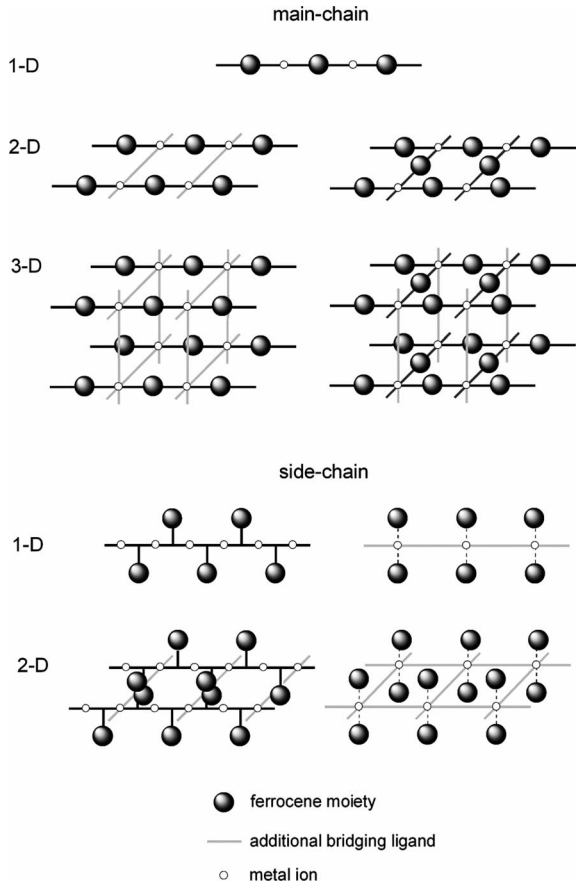


Figure 1. Schematic illustration of the structures of ferrocene-containing coordination polymers.

To date, a number of ferrocene-based ligands and their corresponding metal complexes have been prepared in studies investigating areas such as synthesis, catalysis, and supramolecules, and several books and reviews have been published.[2] This review focuses particularly on the design of ferrocene-containing coordination polymers, offering a novel account of ferrocene-based coordination chemistry. One of the attractive features of these coordination polymers is the structural variety originating from the flexibility of the ligands. This feature, however, makes prediction of the resulting assembled structures difficult, in contrast to the case of coordination polymers with rigid linear bridging ligands. This review covers coordination polymers with basic bidentate ligands such as ferrocenyl pyridines and carboxylates. The design of the ligands and their assembled structures are described in the following section, and the structures and properties of the coordination polymers are described in subsequent sections. A classification of representative ferrocene-containing coordination polymers is given in Tables 1, 2, 3, and 4.

Table 1. Main-chain polymer complexes from neutral ligands.

| Ligand | Topology | Complex | Ref. |
|---|---|---|---|
| DPPF | 1D | $[AuCl(DPPF)]_n$ (**1**) | [6] |
| | | $[AuCl(DPPF)]_n$ (**1′**) | [7] |
| | | $[AuCl(DPPF)]_n$ (**1′′**) | |
| | | $[(AuCl)_2(DPPF)]_n$ (**2**) | [8] |
| | | $[Ag(tfa)(DPPF)]_n$ (**3**) | [9a] |
| | | $[Ag_2(tfa)_2(DPPF)_2{\cdot}H_2O{\cdot}2CH_3CN]_n$ (**3′**) | [9b] |
| | | $[(AuSC_6H_4\{C(=O)N(H)CH_3\})_2(DPPF)]_n$ (**4**) | [10] |
| **L1** | 1D | $[Ag_2(\mathbf{L1})(dppmS_2)_2{\cdot}2ClO_4]_n$ (**5**) | [11] |
| **L2** | 1D | $[CoI_2(\mathbf{L2})]_n$ (**6**) | [12] |
| **L3** | 1D | $[Cu(hfac)_2(\mathbf{L3})]_n$ (**7**) | [5a] |
| | | $[Mn(hfac)_2(\mathbf{L3})]_n$ (**8**) | |
| | | $[Zn(hfac)_2(\mathbf{L3})]_n$ (**9**) | |
| | | $[Ag(\mathbf{L3}){\cdot}PF_6{\cdot}2CH_3CN]_n$ (**10**) | |
| **L4** | 1D | $[Cu(\mathbf{L4}){\cdot}PF_6]_n$ (**11**) | |
| **L5** | 1D | $[CuCl_2(\mathbf{L5})]_n$ (**12**) | [58] |
| | | $[HgBr_2(\mathbf{L5})]_n$ (**13**) | |
| | | $[Ag(CF_3SO_3)(\mathbf{L5})]_n$ (**14**) | |
| **L6** | 1D | $[Ag(\mathbf{L6}){\cdot}ClO_4]_n$ (**15**) | [15] |
| **L7** | 1D | $[Cu_2(PhCOO)_4(\mathbf{L7})]_n$ (**16**) | [19] |
| | | $[Cu_2(C_5H_{11}COO)_4(\mathbf{L7})]_n$ (**17**) | |
| | 2D | $[Cu_2(CH_3COO)_4(\mathbf{L7}){\cdot}\{Cu_2(CH_3COO)_4{\cdot}2H_2O\}]_n$ (**18**) | |
| **L9** | 1D | $[CdBr_2(\mathbf{L9}){\cdot}CH_3OH]_n$ (**26**) | [21] |
| **L10** | 2D | $[HgCl_2(\mathbf{L10})_2]_n$ (**27**) | [22a] |
| **L11** | 1D | $[Cu_2(\mathbf{L11})_2Cl{\cdot}BF_4]_n$ (**28**) | [23] |
| **L12** | 1D | $[Ag(\mathbf{L12}){\cdot}PF_6]_n$ (**29**) | [24] |
| | | $[Ag(\mathbf{L12}){\cdot}PF_6{\cdot}0.5Et_2O]_n$ (**30**) | |
| **L24** | 1D | $[CdBr_2(\mathbf{L24})]_n$ (**89**) | [55a] |
| **L25** | 1D | $[(CdBr_2)_2(\mathbf{L25})_2]_n$ (**90**) | [55b] |

Table 2. Side-chain polymer complexes from neutral ligands.

| Ligand | Topology | Complex | Ref. |
|---|---|---|---|
| **L8** | 1D | $[Cu(hfac)_2(\mathbf{L8})]_n$ (**19**) | [5b] |
| | | $[Mn(hfac)_2(\mathbf{L8})]_n$ (**20**) | |
| | | $[Ni(hfac)_2(\mathbf{L8})]_n$ (**21**) | |
| | | $[Zn(hfac)_2(\mathbf{L8})]_n$ (**22**) | |
| | | $[Cu_2(PhCOO)_4(\mathbf{L8})]_n$ (**23**) | [4b] |
| | | $[Cu_2(C_5H_{11}COO)_4(\mathbf{L8}){\cdot}(CH_3CN)]_n$ (**24**) | |
| | 2D | $[CuI(\mathbf{L8})]_n$ (**25**) | [5b] |
| **L9** | 1D | $[CdBr_2(\mathbf{L9})]_n$ (**31**) | [21] |
| **L12** | 1D | $[Ag_2(\mathbf{L12})_2{\cdot}(tfa)_2{\cdot}2CH_3CN{\cdot}C_6H_6]_n$ (**32**) | [22a] |
| | 2D | $[Ag_2(\mathbf{L12})_2{\cdot}2CF_3SO_3{\cdot}3H_2O]_n$ (**33**) | |

  

Table 3. Main-chain polymer complexes from anionic ligands.

| Ligand | Topology | Complex | Ref. |
|---|---|---|---|
| **L13** | 1D | $[Cd(\mathbf{L13})(H_2O)_3\cdot 4H_2O]_n$ (**34**) | [26] |
| | | $[Cd(\mathbf{L13})(DMF)_2(H_2O)]_n$ (**35**) | [27] |
| | | $[Zn_2(\mathbf{L13})_2(pyridine)_4]_n$ (**36**) | [28] |
| | | $[(SnPh_3)_2(\mathbf{L13})(bpy)]_n$ (**39**) | [29] |
| | | $[(SnPh_3)_2(\mathbf{L13})(bpe)]_n$ (**40**) | |
| | | $[(SnPh_3)_2(\mathbf{L13})(bpp)]_n$ (**41**) | |
| | | $[Cu(tmeda)(\mathbf{L13})]_n$ (**42**) | [30] |
| | | $[Cd(\mathbf{L13})(pebbm)(H_2O)\cdot 2H_2O]_n$ (**52**) | |
| | 2D | $[(Sn(CH_3)_3)_2(\mathbf{L13})]_n$ (**37**) | [29] |
| | | $[(Sn(n\mathrm{Bu})_3)_2(\mathbf{L13})]_n$ (**38**) | |
| | | $[Y_2(\mathbf{L13})_3(H_2O)_4\cdot H_2O]_n$ (**43**) | [26] |
| | | $[Eu_2(\mathbf{L13})_3(H_2O)_4\cdot H_2O]_n$ (**44**) | [31,32] |
| | | $[Eu_2(\mathbf{L13})_3(H_2O)_4\cdot 2H_2O]_n$ (**45**) | [26] |
| | | $[Tb_2(\mathbf{L13})_3(H_2O)_4\cdot 2H_2O]_n$ (**46**) | |
| | | $[Sm_2(\mathbf{L13})_3(H_2O)_4\cdot H_2O]_n$ (**47**) | [33] |
| | | $[Gd_2(\mathbf{L13})_3(CH_3OH)_4\cdot 3H_2O]_n$ (**48**) | [31] |
| | | $[Ce_2(\mathbf{L13})_3(H_2O)_2(CH_3OH)_2\cdot H_2O]_n$ (**49**) | [34] |
| | | $[La_2(\mathbf{L13})_3(CH_3OH)_4]_n$ (**50**) | [31] |
| | | $[Cd(\mathbf{L13})(prbbm)(H_2O)\cdot 3H_2O]_n$ (**53**) | [36] |
| | 3D | $[Cu_2(\mathbf{L13})_2(bbim)_3\cdot 6H_2O]_n$ (**51**) | [35] |

Table 4. Side-chain polymer complexes from anionic ligands.

| Ligand | Topology | Complex | Ref. |
|---|---|---|---|
| **L14** | 1D | $[Sn(o\text{-fluorobenzyl})_3(\mathbf{L14})]_n$ (**54**) | [37] |
| | | $[Na_2Cd(\mathbf{L14})_4(CH_3OH)_2]_n$ (**55**) | [38] |
| | | $[Pb_4(\mathbf{L14})_8(CH_3OH)_2\cdot 3CH_3OH\cdot 2H_2O]_n$ (**56**) | [39] |
| | | $[Zn(\mathbf{L14})_2(bpp)]_n$ (**57**) | |
| | | $[Zn(\mathbf{L14})_2(bbbm)\cdot 2H_2O]_n$ (**58**) | [40] |
| | | $[Zn_2(\mathbf{L14})_4(bpt)_2\cdot 5H_2O]_n$ (**59**) | [39] |
| | | $[Pb(\mathbf{L14})_2(bpe)]_n$ (**60**) | |
| | | $[\{Mn_2(\mathbf{L14})_4\}\{Mn(\mathbf{L14})_2(CH_3OH)_4\}]_n$ (**61**) | [41] |
| | 2D | $[\{Mn_2(\mathbf{L14})_4\}\{Mn(\mathbf{L14})_2(bpy)(H_2O)_2\}]_n$ (**62**) | [41,42] |
| **L15** | 1D | $[UO_2(\mathbf{L15})(THF)\cdot(ferrocene)]$ (**63**) | [43] |
| **L16** | 1D | $[Cd(\mathbf{L16})_2(H_2O)_2\cdot 4H_2O]_n$ (**64**) | [44] |
| | | $[Cd(\mathbf{L16})_2(bbbm)\cdot H_2O]_n$ (**65**) | |
| | | $[Pb(\mathbf{L16})_2(phen)]_n$ (**69**) | |
| | 2D | $[Cd_2(\mathbf{L16})_4(bix)_2\cdot 4CH_3OH]_n$ (**66**) | [45] |
| | | $[Cd_2(\mathbf{L16})_4(btx)_2\cdot 4CH_3OH]_n$ (**67**) | |
| | | $[Cd_2Cl_2(\mathbf{L16})_2(bbbm)_3\cdot 3H_2O]_n$ (**68**) | [44] |
| **L17** | 1D | $[Pb(\mathbf{L17})_2\cdot CH_3OH]_n$ (**70**) | [46] |
| | | $[Zn(\mathbf{L17})_2]_n$ (**71**) | [47] |
| | | $[Zn_2(\mathbf{L17})_4(bpa)\cdot 2CH_3OH]_n$ (**72**) | |
| **L18** | 1D | $[Pb(\mathbf{L18})_2\cdot 2CH_3OH]_n$ (**73**) | [48] |
| | | $[Zn(\mathbf{L18})_2(bpe)]_n$ (**74**) | |
| | | $[Mn(\mathbf{L18})_2(bpy)]_n$ (**75**) | |
| **L19** | 1D | $[Mn(\mathbf{L19})_2(\mu^2\text{-}OH_2)_2(H_2O)_2\cdot H_2O]_n$ (**76**) | [49] |
| | | $[Mn(\mathbf{L19})_2(phen)]_n$ (**77**) | |
| | | $[Cd(\mathbf{L19})_2(prbbm)(H_2O)\cdot H_2O]_n$ (**78**) | [45] |
| | | $[Cd(\mathbf{L19})_2(bpp)\cdot CH_3OH]_n$ (**79**) | [49] |
| | | $[Zn(\mathbf{L19})_2(bbbm)\cdot 3CH_3OH]_n$ (**80**) | [45] |
| **L20** | 1D | $[Cd(\mathbf{L20})_2(bpe)(CH_3OH)_2\cdot 2(H_2O)]_n$ (**81**) | [46] |
| | | $[Zn(\mathbf{L20})_2(bpy)(H_2O)_2\cdot 2(CH_3OH\cdot H_2O)]_n$ (**82**) | |
| | | $[Pb(\mathbf{L20})_2(bpe)]_n$ (**83**) | |
| | | $[Zn(\mathbf{L20})_2(pebbm)]_n$ (**84**) | [50] |
| **L21** | 1D | $[Zn(\mathbf{L21})_2(bpe)]_n$ (**85**) | [51] |
| **L22** | 2D | $[Cd(\mathbf{L22})(bpp)_2\cdot 2CH_3OH\cdot 6H_2O]_n$ (**86**) | [52] |
| | 3D | $[Cd(\mathbf{L22})(bpy)_2\cdot 4CH_3OH]_n$ (**87**) | |
| **L23** | 2D | $[Zn(\mathbf{L23})_2(bpy)_2]_n$ (**88**) | [53] |

## Ferrocene-Containing Ligands and Modes of Assembly

### Ferrocene-Containing Ligands for Coordination Polymers

This section reviews the design and features of basic ferrocene-containing ligands that provide coordination polymers. The ligands include 1,1′-disubstituted and monosubstituted ferrocenes with *P*-, *N*-, *S*-, and *O*-donor substituents (Figure 2). In 1,1′-disubstituted ferrocenes, the torsion angle $\tau$ is used to express the conformation (Figure 3), and the conformational flexibility of the Cp rings provides the coordination polymers with structural variety. The parameter $\tau$ is defined as the torsion angle of $X^1$–$Cp^1$–$Cp^2$–$X^2$, where $X^1$ and $X^2$ are carbon atoms bearing substituents, and $Cp^1$ and $Cp^2$ are the centroids of the Cp rings.[2]

1,1′-Bis(diphenylphosphanyl)ferrocene, abbreviated as DPPF (Figure 2a), is a well-known example of a ferrocene-containing bidentate ligand.[2] The ligand usually chelates to metal ions to give discrete complexes, but several coordination polymers with DPPF and related ligands are known.[6–10] $DPPFE_2$ [E = S (**L1**), O (**L2**)] can coordinate to metal ions via the chalcogen atoms, providing a building block for coordination polymers.[11,12] DPPF was one of the first ligands used in a ferrocene-containing coordination polymer, reported as early as 1989.[9] Most complexes with other ligands have been reported since 2002.

Ferrocenes with bis(thioether) substituents can be prepared conveniently by the reaction of 1,1′-dilithioferrocene with disulfides.[4a,13–16] Ligands **L3**, **L4**, and **L5** link metal ions via the *N*-donor moiety,[5a,13,14] while **L6** bridges them via the thioketone moiety, to form 1D coordination polymers.[15] Derivatives with no such additional donor sites, such as 1,1′-bis(phenylthio)ferrocene, lead to discrete complexes in which the thioether moieties coordinate to metal ions.[16] Ligand **L3** cannot chelate to a metal ion via the *N*-donor moiety, but **L4** can coordinate in chelate fashion to form discrete complexes.[14]

Ferrocene derivatives with heteroaryl substituents are known to be versatile ligands. For example, pyridylferrocenes[17] and 1,1′-bis(pyridyl)ferrocenes[18] are well-known ligands, but their coordination polymers have not been reported. 1,1′-Bis(2-pyridyl)ferrocene[18a,18b] affords chelate complexes governed by steric hindrance around the donor atom, while 1,1′-bis(4-pyridyl)ferrocene[18c] affords macrocyclic metal complexes in which the ligand adopts a synperiplanar conformation ($\tau \approx 0°$), exhibiting an intramolecular π···π interaction between the substituents. In contrast, 1,1′-bis(pyrazinyl)ferrocene (**L7**) provides coordination polymers as well as macrocyclic complexes, because the two pyrazine rings may lie in either the same direction or different directions (Figure 4).[19] Ferrocenylpyrimidine (**L8**) is a monosubstituted ferrocene carrying a bidentate moiety, which was designed to produce side-chain coordination polymers, as pyrimidine gives 1D coordination polymers.[4b,5b,19]

Even though 1,1′-bis(azaheterocyclic) ferrocenes carrying flexible spacer groups tend to produce discrete metallacyclic complexes;[20] several coordination polymers have been reported. Complexes derived from **L9**[21] and **L10**[22] show structural diversity due to the conformational flexibility and hydrogen-bonding ability of the spacer groups. Ligand **L10** is less flexible and its substituents tend to be parallel with each other, as also observed in complexes with 1,1′-bis(4-pyridyl)ferrocene and **L7**. Ligand **L11**[23] behaves

  

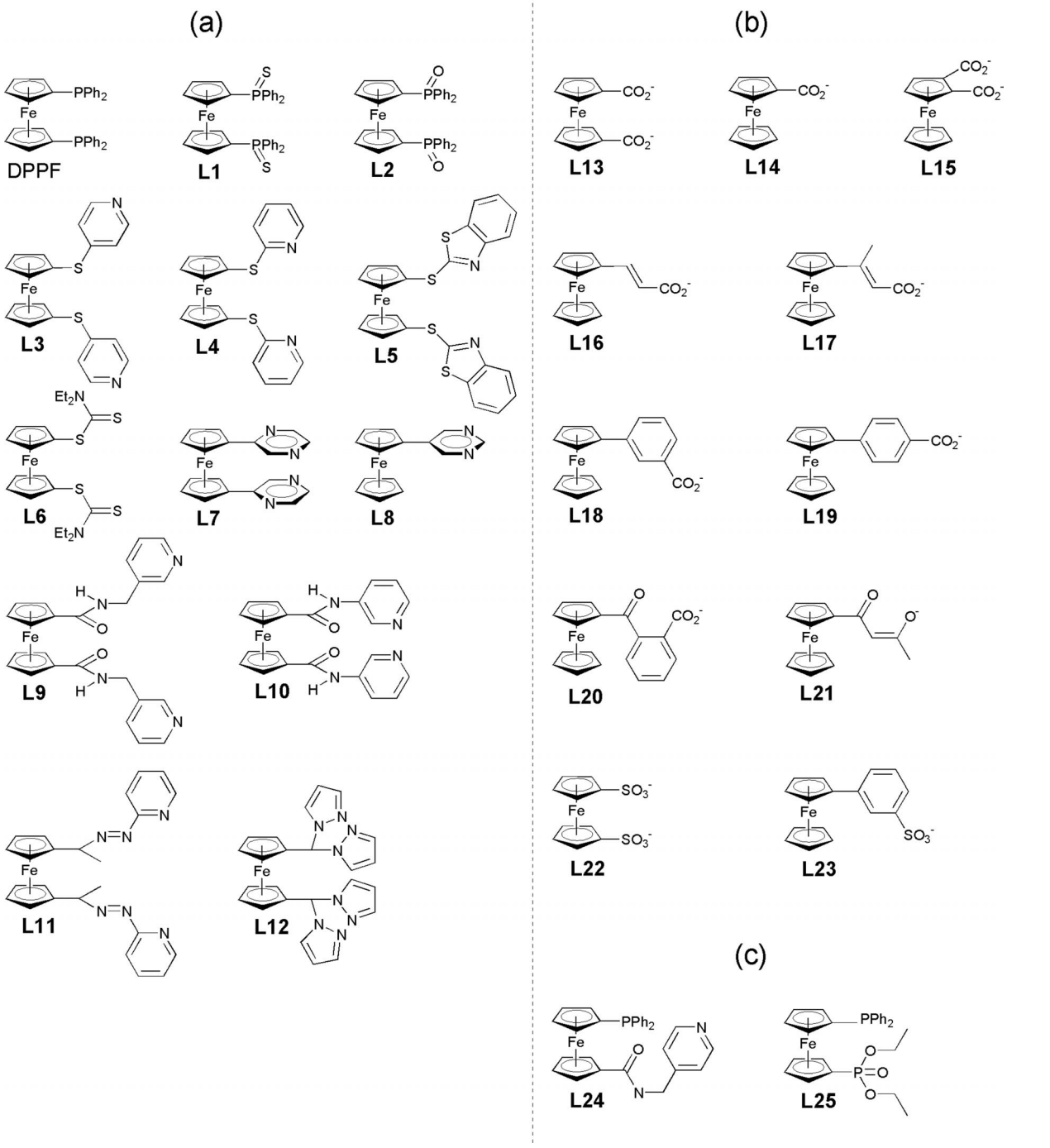


Figure 2. Ferrocene-containing ligands used for the preparation of ferrocene-containing coordination polymers: (a) neutral ligands, (b) anionic ligands, and (c) unsymmetrical neutral ligands.

as a chelate-bridging ligand. Ligand **L12**,[24] which carries bis(pyrazolyl)methane coordination sites, is an important chelate-bridging ligand, affording typical 1D main-chain coordination structures.

In addition to the neutral ligands described above, anionic ligands with *O*-donor substituents are also versatile (Figure 2b). Carboxylated ferrocenes **L13**–**L20** produce coordination polymers with more complicated structures, because of the multidentate character of the carboxylate moiety.[25] These anionic ligands lead to higher-dimensional structures when an additional bridging ligand is introduced.[26–50] Coordination polymers are also obtained from chelating ligand **L21** and sulfonated ferrocenes **L22** and **L23** in the presence of additional bridging ligands.[51–53] Ligand **L22** behaves not as a chelating ligand but as a bridging one. These anionic ligands may also behave as counteranions, giving structural versatility to the coordination polymers.

  

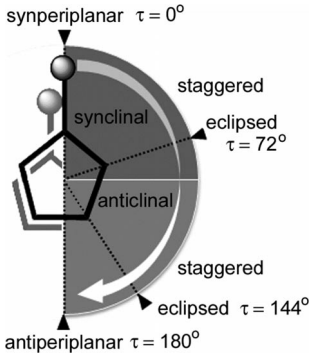


Figure 3. Conformational freedom in 1,1′-disubstituted ferrocenes. The torsion angle $X^1$–$Cp^1$–$Cp^2$–$X^2$ is defined as $\tau$.

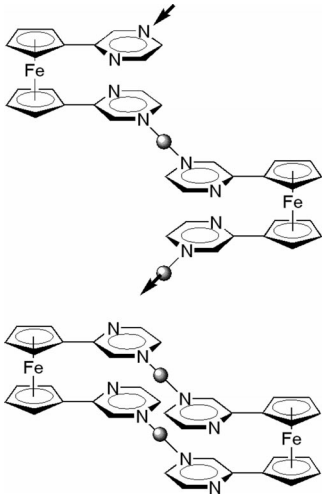

Figure 4. Conformations of synperiplanar 1,1′-bis(pyrazinyl)ferrocene in its metal complexes: (a) coordination polymers and (b) metallamacrocycles.

While we have discussed symmetrical ferrocene ligands, 1,1′-unsymmetrically substituted ferrocenes **L24** and **L25** (Figure 2c) also form main-chain coordination polymers. Such ligands are particularly interesting, because they carry donor atoms with different donor abilities, and may lead to different coordination structures depending on the hardness of the metal ions. Although there are many unsymmetrical ferrocene ligands with mixed donor atoms, examples of their coordination polymers are limited, because such ligands generally adopt a chelate coordination mode, generating discrete complexes with metal salts.[54,55a]

Many of the ligands shown above afford not only coordination polymers but also hydrogen-bonded network complexes when combined with hydrogen-bond donors or acceptors instead of metal salts.[2a,56] These hydrogen-bonded assemblies are interesting and structurally relevant to coordination polymers, but they are outside the scope of this review.

## Design and Structures of Ferrocene-Containing Coordination Polymers

Ferrocene-containing coordination polymers are mostly one-dimensional (1D). In this section, the design of the assembled structures of ferrocene-based coordination polymers is discussed in comparison with conventional ferrocene-containing polymers.

Conventional main-chain ferrocene polymers are often prepared by condensation polymerization. For example, the reaction of 1,1′-difunctionalized ferrocenes containing leaving groups with an appropriate diol produces main-chain polymers (Scheme 1a).[3f] Preparation of the corresponding main-chain coordination polymers is analogous (Scheme 1b): 1,1′-disubstituted ferrocenes carrying donor moieties (DPPF, **L1**–**L7**, **L9**–**L13**, **L22**, **L24**, **L25**) react with metal ions with two coordination sites to give main-chain coordination polymers. The shape of the 1D chain in the coordination polymer varies from linear to zigzag with decreasing torsion angle $\tau$ (Figure 5). Therefore, ferrocene-containing coordination polymers are more flexible than

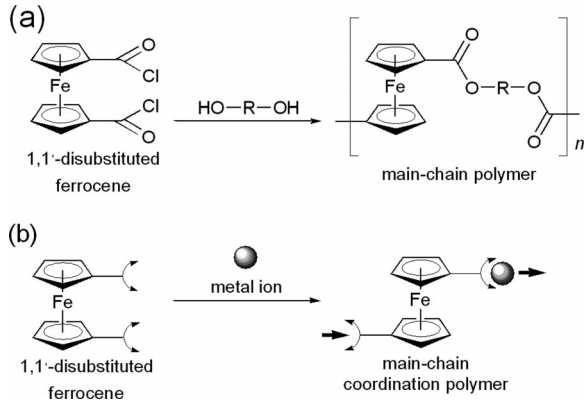


Scheme 1. Preparation of main-chain ferrocene-containing polymers. Examples of (a) a conventional polymer and (b) a coordination polymer.

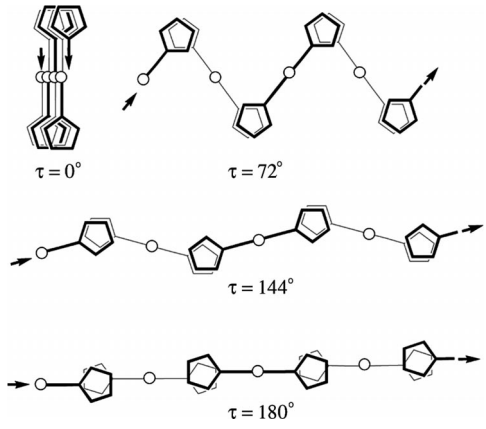


Figure 5. Structural variations in 1D main-chain ferrocene-containing coordination polymers depending on the torsion angle $\tau$.

  

other types of coordination polymers, in that they can bend not only at the metal nodes but also at the bridging ferrocenyl moieties. In addition, variation in the torsion angle between the substituents and the Cp rings adds further structural diversity.[6–10,22]

Conventional side-chain ferrocene polymers are generally prepared by polymerization of monosubstituted ferrocenes.[3] Scheme 2a shows an example of radical polymerization, which affords homopolymers and copolymers. The tacticity of the product is usually not regular, and the monomer sequence is random.[3g] In contrast, stereoregular ferrocene-containing side-chain coordination polymers are obtained by the reaction of metal salts and monosubstituted ferrocenes with bidentate sites (**L8**, **L14**, **L16**–**L21**, **L23**) (Scheme 2b).

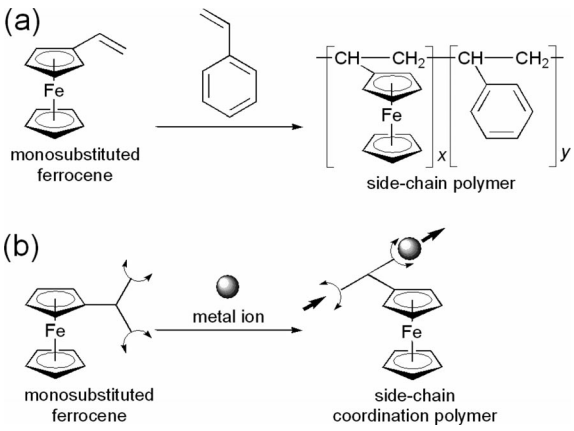


Scheme 2. Preparation of side-chain ferrocene-containing polymers. Examples of (a) a conventional polymer and (b) a coordination polymer.

In addition to these coordination polymers, higher-dimensional coordination polymers can be formed by introducing an additional bis(*N*-donor) bridging ligand (Figure 6) for the carboxylate complexes.[29,35,36,39–42,44–50] When the additional ligand is introduced, the carboxylate anion changes coordination mode, and the metal center accepts the additional ligand, leading to a high-dimensional coordination polymer (Figure 1).[29]

The preparation of these coordination polymers is mostly straightforward. Those with neutral ligands (DPPF, **L1**–**L12**, **L24**, **L25**) are prepared by reactions of the ligands and metal salts, while those with anionic ligands (**L13**–**L23**) are prepared by metathesis reactions between the alkaline salt of the ligand and transition metal salts such as halides, nitrates, and acetates. Mixed-ligand coordination polymers are obtained either by adding bridging ligands to these complexes or by the reaction of free acid ligands, metal salts, and additional ligands. It is to be noted that metal complexes sometimes undergo transformations in solution, producing solvent-dependent products.[4b,5a,6,7,21]

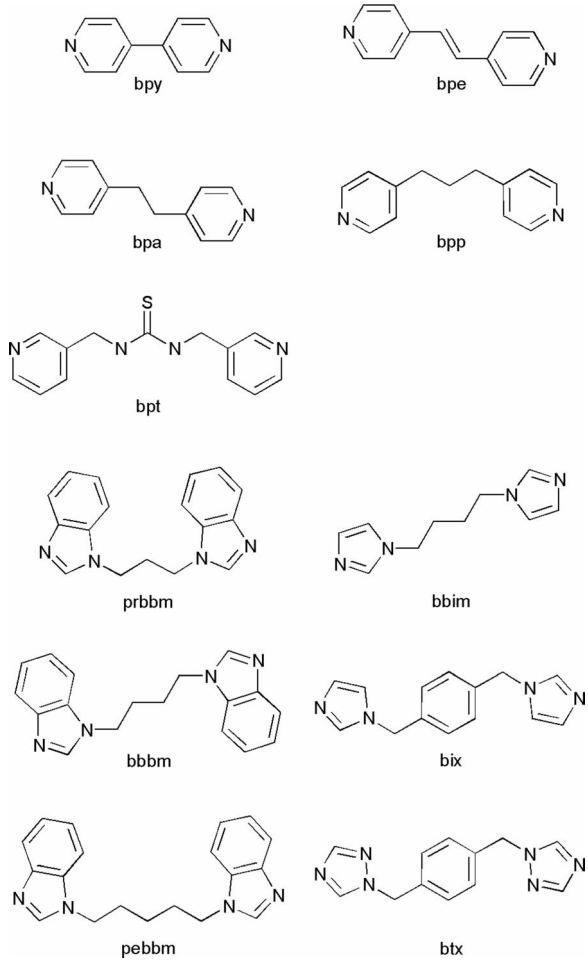


Figure 6. Bis(*N*-donor) bridging ligands that act as additional ligands.

## Coordination Polymers from Diphenylphosphanylferrocenes

DPPF and related ligands produce main-chain coordination polymers. Among these, $[AuCl(DPPF)]_n$ complexes are an example of supramolecular isomerism[57] associated with the conformational flexibility of the ferrocenyl ligand. The complex has three crystal modifications. Polymorph **1** is prepared by conversion of a 2:1 M/L complex, $[(AuCl)_2(DPPF)]_n$, in $CDCl_3$ (Figure 7a).[6] Polymorphs **1′** (Figure 7b) and **1′′** (Figure 7c) are prepared by the same reaction in $CH_2Cl_2$.[7] These are 1D coordination polymers composed of alternating DPPF and AuCl units, in which the $Au^I$ metal centers exhibit planar trigonal coordination geometries. The values of $\tau$ are around 150°, 180°, and 130° for **1**, **1′**, and **1′′**, respectively, accompanied by varying intrachain Au···Au separations of 6.58, 8.36, and 8.55 Å, respectively. Thus, the flexibility of the 1D chain leads to structural differences. Interestingly, the 2:1 M/L complex $[(AuCl)_2(DPPF)]_n$ (**3**) is also a 1D coordination polymer (Figure 7d).[8] In this complex, two crystallographically independent $(AuCl)_2(DPPF)$ units with different $\tau$ values ($\tau \approx$ 180° and 150°) alternate. The $(AuCl)_2$ unit features an Au···Au interaction distance of 3.08 Å.

  

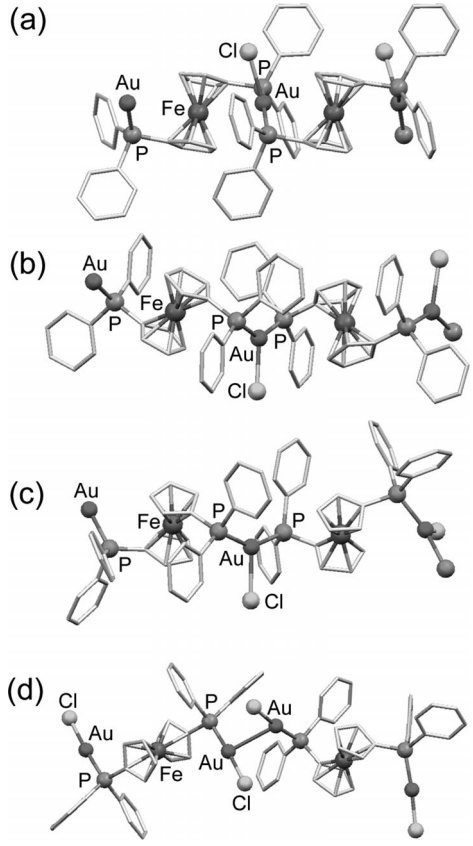


Figure 7. 1D chain structures of (a) $[AuCl(DPPF)]_n$ (**1**), (b) $[AuCl(DPPF)]_n$ (**1′**), (c) $[AuCl(DPPF)]_n$ (**1′′**), and (d) $[(AuCl)_2(DPPF)]_n$ (**3**).

Silver complexes $[Ag(tfa)(DPPF)]_n$ (**3**)[9a] and $[Ag_2(tfa)_2(DPPF)_2{\cdot}H_2O{\cdot}2CH_3CN]_n$ (**3′**)[9b] (tfa = trifluoroacetate) are structurally similar to **1′** and **1′′**, respectively. The major differences between **3** and **3′** are in the $\tau$ values of DPPF (180° for **3** and 123° for **3′**) and the coordination environments around the $Ag^I$ center. The $Ag^I$ ion in **3** adopts a tetrahedral geometry, coordinated by two phosphorus atoms from two different DPPF ligands and two oxygen atoms from chelating tfa molecules, while that in **3′** possesses a T-shaped geometry formed by two phosphorus atoms and one monodentate tfa. $[Ag(tfa)(DPPF)]_n$ (**3**) is prepared by the reaction of the discrete $[Ag_2(tfa)_2(DPPF)]$ complex with 1 mol equiv. of DPPF.[9a]

The DPPF derivative **L1** produces a 1D coordination polymer, $[Ag_2(\mathbf{L1})(dppmS_2)_2{\cdot}2ClO_4]_n$ (**5**) [$dppmS_2$ = bis(diphenylthiophosphanyl)methane] (Figure 8a), in which the $Ag_2(dppmS_2)_2$ units are linked by the antiperiplanar **L1** ligand ($\tau \approx 180°$).[11] The reaction of **L1** with $AgClO_4$ gives 1:1, 1:2, and 2:1 M/L complexes, and compound **5** is produced by the reaction of the 1:1 complex $[Ag(\mathbf{L1}){\cdot}ClO_4]$ with $dppmS_2$. Another 1D coordination polymer worth mentioning is $[CoI_2(\mathbf{L2})]_n$ (**6**) (Figure 8b), which contains antiperiplanar **L2** ($\tau \approx 180°$).[12] This complex is obtained by air oxidation of $[(Cp)CoI_2(DPPF)]^+I^-$ and not by direct reaction of **L2** with $CoI_2$.

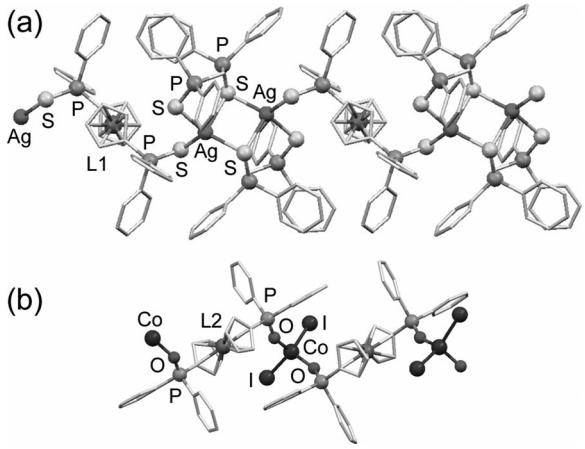


Figure 8. 1D chain structure of (a) $[Ag_2(\mathbf{L1})(dppmS_2)_2{\cdot}2ClO_4]_n$ (**5**) and (b) $[CoI_2(\mathbf{L2})]_n$ (**6**).

## Coordination Polymers from Ferrocenes with Thioether Substituents

Main-chain coordination polymers can be prepared from thioether-substituted ferrocenes **L3**–**L6**. In complexes with **L3**, the twist of the 1D chain is affected by the M···M interaction of the bridging metals. $[M(hfac)_2(\mathbf{L3})]_n$ [$M^{II}$ = Cu (**7**), Mn (**8**), Zn (**9**)] (hfac = 1,1,1,5,5,5-hexafluoroacetylacetonate) consists of alternate arrangements of antiperiplanar **L3** ($\tau \approx 180°$) and *trans*-$[M(hfac)_2]$, forming straight-chain coordination polymers (Figure 9a).[4a] $[Ag(\mathbf{L3}){\cdot}PF_6{\cdot}2CH_3CN]_n$ (**10**) is also a 1D coordination polymer (Figure 9b), but the ferrocene moieties are located on one side of the chain ($\tau = 40°$).[4a] This is associated with the "argentophilic" intrachain Ag···Ag interaction. The $Ag^I$ ion adopts a linear geometry, coordinated with two nitrogen atoms from two **L3** ligands. In addition, these complexes show interesting physical properties such as redox activity.

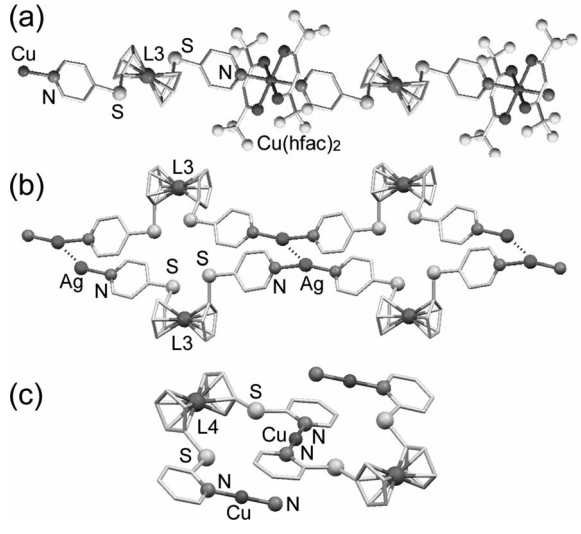


Figure 9. 1D straight-chain structures of (a) $[Cu(hfac)_2(\mathbf{L3})]_n$ (**7**), (b) $[Ag(\mathbf{L3}){\cdot}PF_6{\cdot}2CH_3CN]_n$ (**10**), and (c) 1D twisted zigzag structure of $[Cu(\mathbf{L4}){\cdot}PF_6]_n$ (**11**). Dashed lines in (b) indicate Ag···Ag argentophilic interactions.

  

Solid-state cyclic voltammograms for **7** and **10** show redox waves at 0.39 and 0.42 V (vs. ferrocene-ferrocenium), respectively, which may be ascribed to the redox processes of the ferrocenyl moiety.[4a] Complexes **7** and **8** are paramagnetic as a result of the presence of magnetic ions.

Comparison of these complexes of **L3** with those of **L4** shows how the twist in the chain structure depends on the ligand positional isomer. Although the complexes with **L3** (**7**–**10**) exhibit straight-chain structures, isomer **L4** forms a highly twisted chain complex $[Cu(\mathbf{L4})\cdot PF_6]_n$ (**11**) with $\tau$ = 38° (Figure 9c).[4a] This complex is obtained as air-sensitive crystals by the reaction of **L4** and $[Cu(CH_3CN)_4]PF_6$. The $Cu^I$ ions are arranged linearly and are separated from each other by approximately 4.0 Å.

$[CuCl_2(\mathbf{L5})]_n$ (**12**), $[HgBr_2(\mathbf{L5})]_n$ (**13**), and $[Ag(CF_3SO_3)(\mathbf{L5})]_n$ (**14**) form different structures (Figure 10) due to the conformational flexibility of the substituents and the different coordination environments of the metal ions.[58] In these complexes, the ligand acts as a bridging bidentate ligand ($\tau \approx 180°$), coordinating to the "hard" and "soft" metal ions through the "hard" *N*-donor atoms. Complex **12** shows a zigzag structure in which the $Cu^{II}$ center adopts a square-planar geometry (Figure 10a), while **13** consists of a twisted zigzag structure in which the $Hg^{II}$ center is in a highly distorted tetrahedral geometry (Figure 10b). $[ZnCl_2(\mathbf{L5})]_n$ exhibits a structure similar to that of **13**. The chain structure of **14** is highly twisted, containing two conformationally different **L5** ligands in the chain (Figure 10c).

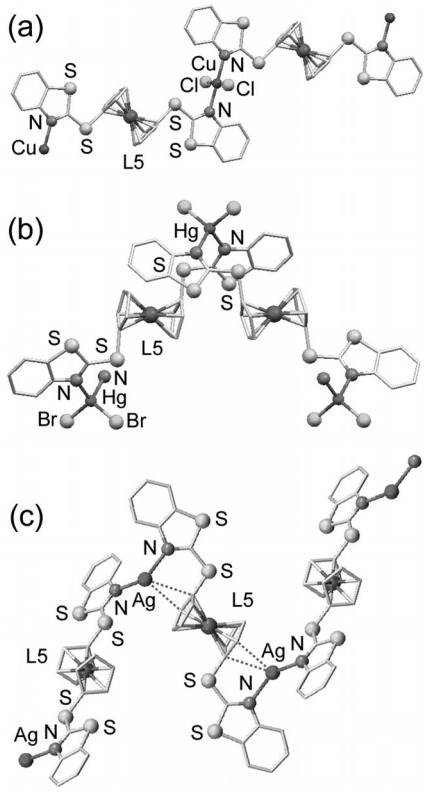


Figure 10. 1D chain structure of (a) $[CuCl_2(\mathbf{L5})]_n$ (**12**), (b) $[HgBr_2(\mathbf{L5})]_n$ (**13**), and (c) $[Ag(CF_3SO_3)(\mathbf{L5})]_n$ (**14**). Dashed lines in (c) indicate Ag···π interactions.

The silver center in **14** is coordinated with two nitrogen atoms from the ligands and one oxygen atom from the counteranion and has an additional contact with the cyclopentadienyl ring in a $\eta^2$ fashion (Ag···C ≈ 2.9 Å), forming a trinuclear sandwiched coordination structure.

Ligand **L6** exhibits an interesting coordination mode in $[Ag(\mathbf{L6})\cdot ClO_4]_n$ (**15**), which contains an alternating arrangement of antiperiplanar **L6** ($\tau \approx 180°$) and $Ag^I$ ions (Figure 11).[15] The silver centers are coordinated with two sulfur atoms of different ferrocene moieties and also with the cyclopentadienyl rings in a $\eta^2$ fashion, giving a double-sandwich assembled structure.

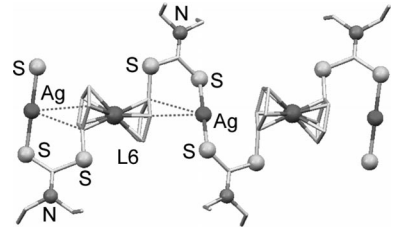


Figure 11. 1D double-sandwich assembled structure of $[Ag(\mathbf{L6})\cdot ClO_4]_n$ (**15**). Dashed lines indicate Ag···π interactions.

## Coordination Polymers from Heteroaryl Ferrocenes

### Main-Chain Coordination Polymers

Ligand **L7** produces main-chain coordination polymers as well as discrete complexes, and these examples show how the bulkiness of the bridging metal-containing species affects the assembled structures. $Ag^I$ complexes with **L7** are macrocyclic discrete complexes with $\tau \approx 0°$, as shown in Figure 12a,[19] but $Cu^{II}$ carboxylate complexes with **L7**, $[Cu_2(RCOO)_4(\mathbf{L7})]_n$ [R = Ph (**16**) (Figure 12b), $C_5H_{11}$ (**17**)], are 1D coordination polymers with step-like structures, composed of an alternating arrangement of Cu dinuclear lantern units and synperiplanar **L7** ($\tau \approx 0°$).[19] $[Cu_2(CH_3COO)_4(\mathbf{L7})\cdot\{Cu_2(CH_3COO)_4\cdot 2H_2O\}]_n$ (**18**) contains the same step-like $[Cu_2(RCOO)_4(\mathbf{L7})]_n$ chains, which are further hydrogen-bonded via the additional dinuclear lantern unit $[Cu_2(CH_3COO)_4(H_2O)]$ to form a 2D sheet structure (Figure 12c). There is a hydrogen bond between the non-coordinating *N*-donor moiety of **L7** in the chain and the coordinating water molecule of the interchain dinuclear unit.[19] In these $Cu^{II}$ complexes, the steric hindrance of the dinuclear unit prevents the formation of macrocyclic complexes, leading to the formation of coordination polymers.

### Side-Chain Coordination Polymers

Ligand **L8** gives ideal 1D side-chain polymers based on its rational design. These are interesting from the point of view of magnetism. The polymers $[M(hfac)_2(\mathbf{L8})]_n$ [$M^{II}$ = Cu (**19**), Mn (**20**), Ni (**21**), and Zn (**22**)] are isomorphous coordination polymers comprising a 1D chain structure

  

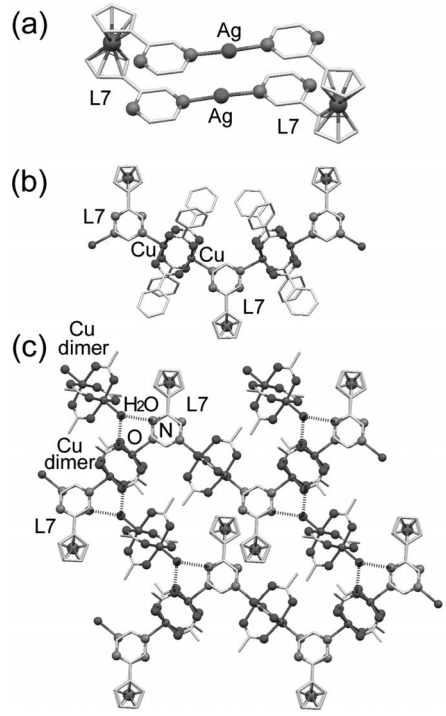


Figure 12. (a) Macrocyclic structure of $Ag^{I}$ complexes with **L7**; 1D step-like structures of (b) $[Cu_2(PhCOO)_4(\mathbf{L7})]_n$ (**16**) and (c) $[Cu_2(CH_3COO)_4(\mathbf{L7})\cdot\{Cu_2(CH_3COO)_4\cdot 2H_2O\}]_n$ (**18**).

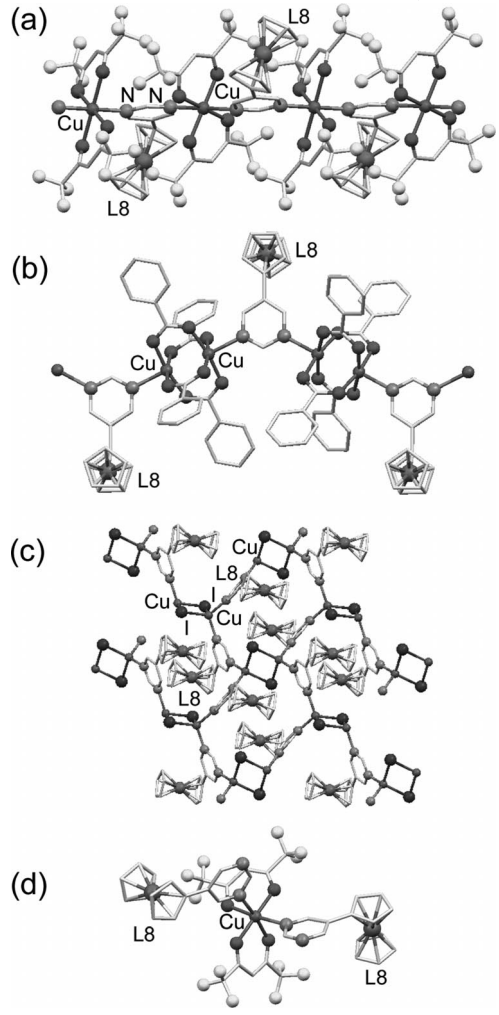


Figure 13. 1D chain structures of (a) $[Cu(hfac)_2(\mathbf{L8})]_n$ (**19**), (b) $[Cu_2(PhCOO)_4(\mathbf{L8})\cdot(guest)]_n$ (**23**), (c) 2D sheet structure of $[CuI(\mathbf{L8})]_n$ (**25**), and (d) 1:2 M/L discrete complex with **L8**.

that contains an alternating arrangement of *trans*-[M(hfac)$_2$] and **L8** (Figure 13a).[4b] Lantern-like dinuclear copper carboxylates also give 1D coordination polymers $[Cu_2(RCOO)_4(\mathbf{L8})\cdot(guest)]_n$ [R = Ph, guest = none (**23**) (Figure 13b); R = $C_5H_{11}$, guest = $CH_3CN$ (**24**)].[5b] The use of a copper halide leads to an extended structure. The reaction of **L8** with CuI gives a 2D network complex $[CuI(\mathbf{L8})]_n$ (**25**), in which $[Cu_2I_2]$ units connect the ligands (Figure 13c).[4b] Investigation of the magnetic properties of **19** shows that the $Cu^{II}$ ions ($s$ = 1/2) are at equal separation, forming a 1D chain structure with a Cu···Cu distance of 6.0 Å. Coordination polymers of pyrimidine derivatives are of interest due to their potential for molecular magnetism, because the magnetic interaction between the copper ions becomes ferromagnetic for axial–axial and axial–equatorial coordination modes.[59] In **19**, weak antiferromagnetic interactions ($2J$ = –6.3 K) are observed between the $Cu^{II}$ ions. In this complex, the pyrimidine moiety coordinates to one $Cu^{II}$ ion in equatorial–equatorial and to the other in axial–axial fashion, which is the origin of the antiferromagnetic behavior. Although small, this intrachain interaction is significant when compared with the negligible intermolecular magnetic interactions in the main-chain coordination polymer $[Cu(hfac)_2(\mathbf{L3})]_n$ (**7**) (Weiss temperature $\theta$ = –0.06 K).[4a] In addition, these coordination complexes have been shown to exhibit redox processes in the solid state based on the redox activity of the ferrocenyl group.

The choice of solvent is crucial for the complexion of **L8** with [M(hfac)$_2$]. The reaction in pentane gives a 1:1 M/L coordination polymer, while the reaction in diethyl ether affords discrete 1:2 M/L complexes (Figure 13d), regardless of the amount of ligand present.[5a] In these discrete complexes, **L8** acts as a monodentate ligand, coordinating to the metal ion through one of the two nitrogen atoms and leaving the other one free. Interestingly, this corresponds to isolation of the local structure of the 1:1 M/L coordination polymer.

## Coordination Polymers from Azaheterocyclic Ferrocenes with Spacer Groups

### Main-Chain Coordination Polymers

The reaction of **L9** and $CdBr_2$ in a methanol solution gives rise to $[CdBr_2(\mathbf{L9})\cdot CH_3OH]_n$ (**26**), which exhibits a repeated rhomboidal structure (Figure 14).[21] The rhomboid is composed of two $Cd^{II}$ ions with a distorted octahedral geometry and two **L9** molecules with an anticlinal conformation. The structures of $[MX_2(\mathbf{L10})_2]_n$ (M = Zn, Cd, Hg; X = Cl, Br, SCN, $N_3$, $NO_3$) are similar to each other.[22a]

  

The structure of $[HgCl_2(\mathbf{L10})_2]_n$ (**27**) is shown in Figure 15 as a representative example. The complex has a waved 2D structure, composed of a macrocyclic unit $[Hg_4(\mathbf{L10})_4]$, in which the $Hg^{II}$ ion exhibits an octahedral geometry, coordinated with two axial chloride ligands and four equatorial nitrogen atoms from four **L10** ligands. The ligand adopts a synperiplanar conformation ($\tau \approx 0°$), the nitrogen atoms of the pyridine rings pointing in different directions to serve as a bridging module.[22a] Complexes with **L11** exhibit chelate coordination. $[Cu_2(\mathbf{L11})_2Cl{\cdot}BF_4]_n$ (**28**) exhibits a double-helicate structure (Figure 16), in which dimeric $[Cu_2(\mathbf{L11})_2]$ units are bridged by $\mu^2$ chloride ions.[23] The dimer unit is composed of two $Cu^{II}$ ions with trigonal bipyramidal geometry and two **L11** ligands with an anticlinal conformation, stabilized by intermolecular π···π interactions between the pyridine ring and the Cp ring.

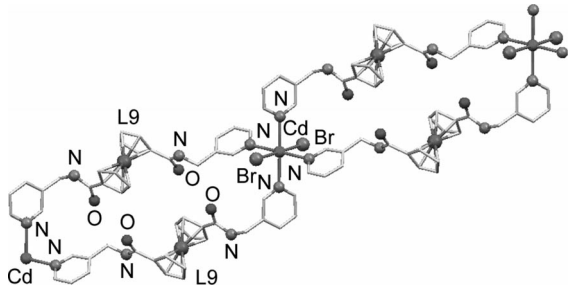


Figure 14. 1D repeated rhomboidal structure of $[CdBr_2(\mathbf{L9}){\cdot}CH_3OH]_n$ (**26**).

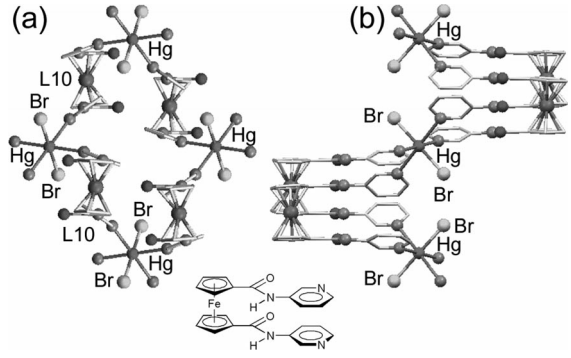


Figure 15. 2D sheet structure of $[HgCl_2(\mathbf{L10})_2]_n$ (**27**); (a) along the *a* axis and (b) along the *c* axis.

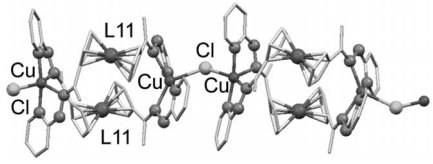


Figure 16. 1D chain structure of $[Cu_2(\mathbf{L11})_2Cl{\cdot}BF_4]_n$ (**28**).

**L12** acts as a chelate-bridging ligand. The reactions of **L12** and $Ag^I$ salts lead to 1D coordination polymers $[Ag(\mathbf{L12}){\cdot}X{\cdot}(solvent)]_n$ (X = $BF_4^-$, $PF_6^-$, $CF_3SO_3^-$, or $SbF_6^-$; solvent = none, $0.5Et_2O$, or $1.5C_6H_6$).[24] The complexes with and without solvent molecules possess zigzag and helical chain structures, respectively. As examples, structures of the helical complex $[Ag(\mathbf{L12}){\cdot}PF_6]_n$ (**29**) and the zigzag complex $[Ag(\mathbf{L12}){\cdot}PF_6{\cdot}0.5Et_2O]_n$ (**30**) are shown in Figures 17a and 17b, respectively. The difference in their structure originates from the axial chirality[1c] of the ligand around the $Cp^1$–Fe–$Cp^2$ axis: the helical chain in **29** consists of ligands with the same chirality, while the zigzag chain in **30** is composed of an alternate arrangement of the *R* and *S* enantiomers.

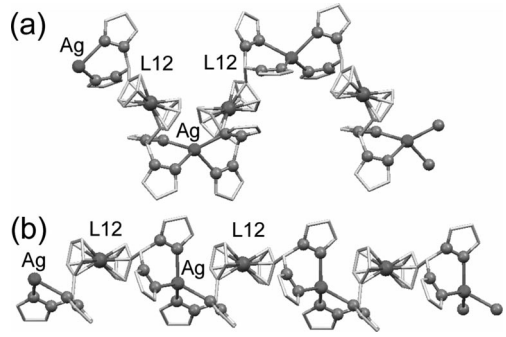


Figure 17. 1D chain structures of (a) $[Ag(\mathbf{L12}){\cdot}PF_6]_n$ (**29**) and (b) $[Ag(\mathbf{L12}){\cdot}PF_6{\cdot}0.5Et_2O]_n$ (**30**).

## Side-Chain Coordination Polymers

The reaction of **L9** and $CdBr_2$ in DMF/$Et_2O$ solution leads to a side-chain polymer $[CdBr_2(\mathbf{L9})]_n$ (**31**) (Figure 18),[21] in contrast to the main-chain polymer **29** ($[CdBr_2(\mathbf{L9}){\cdot}CH_3OH]_n$). The polymer backbone in **31** consists of $[CdBr_2]_n$, which are chelated by **L9**. Each chain involves two different **L9** ligands that are mirror images of each other. The ligand exhibits intramolecular NH···O=C hydrogen bonding between the 1- and 1′-substituents.

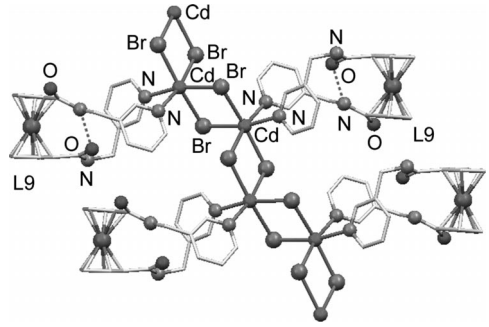


Figure 18. 1D chain structure of $[CdBr_2(\mathbf{L9})]_n$ (**31**).

Metal complexes with **L10** tend to adopt metallamacrocyclic structures similar to those found in 1,1′-bis(4-pyridyl)ferrocene and **L7**, which are linked by additional interactions to construct 1D coordination polymers. $[Ag_2(\mathbf{L10})_2{\cdot}(tfa)_2{\cdot}2CH_3CN{\cdot}C_6H_6]_n$ (**32**) (Figure 19a) is a ladder-like coordination polymer, in which the macrocyclic dimers are linked via an interdimer Ag–O bond. Ligand **L10** adopts a synperiplanar conformation ($\tau \approx 0°$) with the *N*-donor moieties of each pyridine ring arranged in the same direction.[22a] $[Ag_2(\mathbf{L10})_2{\cdot}2CF_3SO_3{\cdot}3H_2O]_n$ (**33**) (Figure 19b) is a

  

2D coordination polymer, in which the macrocyclic dimers are linked via interdimer Ag···Cp interactions, giving a double sandwich structure.[22a]

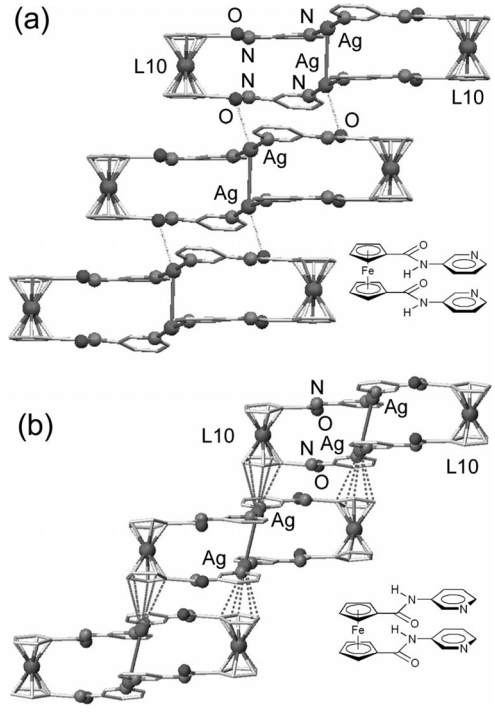


Figure 19. 1D ladder-like structures of (a) $[Ag_2(\mathbf{L10})_2 \cdot (tfa)_2 \cdot 2CH_3CN \cdot C_6H_6]_n$ (**32**) and (b) $[Ag_2(\mathbf{L10})_2 \cdot 2CF_3SO_3 \cdot 3H_2O]_n$ (**33**). Dashed lines in (b) indicate Ag···π interactions.

## Coordination Polymers from Carboxylated Ferrocenes

### Main-Chain Coordination Polymers

Because of the multidentate coordination properties of the carboxylate moiety, **L13** produces 1D main-chain coordination polymers with rather complicated local structures. $[Cd(\mathbf{L13})(H_2O)_3 \cdot 4H_2O]_n$ (**34**) and $[Cd(\mathbf{L13})(DMF)_2(H_2O)]_n$ (**35**) exhibit zigzag chain structures, twisted differently depending on $\tau$ ($\tau$ = 60° for **34** and 133° for **35**) (Figures 20a and 20b).[26,27] $[Zn_2(\mathbf{L13})_2(pyridine)_4]_n$ (**36**) exhibits a 1D ribbon-like structure ($\tau$ = 113°) (Figure 20c), in which one of the two carboxylate groups of **L13** coordinates to the $Zn^{II}$ center in a monodentate fashion while the other bridges two $Zn^{II}$ ions in a *syn-anti* bridging mode.[28]

Complexes $[(SnR_3)_2(\mathbf{L13})]_n$ [R = Me (**37**; Figure 21a), *n*Bu (**38**)] exhibit 2D sheet structures and are isostructural with each other, while $[(SnPh_3)_2(\mathbf{L13})]$ is a discrete complex.[29] These are interesting examples with organometallic components. The 2D sheet structure in **37** and **38** is composed of repeated macrocycles with four $SnR_3$ and four **L13** units, in which **L13** adopts an anticlinal conformation ($\tau$ = 109°) and links four Sn atoms in a *syn-anti* bridging mode. Addition of *N*-donor ligands lead to 1D coordination polymers $[(SnPh_3)_2(\mathbf{L13})(L–L)]_n$ [L–L = bpy (**39**), bpe (**40**; Figure 21b), bpp (**41**)], which are composed of an alternate arrangement of $(Ph_3Sn)$–μ-**L13**–$(SnPh_3)$ and L–L units.[29] In these complexes, **L13** adopts an antiperiplanar conformation ($\tau \approx 180°$) and coordinates to the metal in a monodentate mode, while that in precursor $[(SnPh_3)_2(\mathbf{L13})]$ has a synclinal conformation ($\tau$ = 71°) with a bidentate coordination mode.

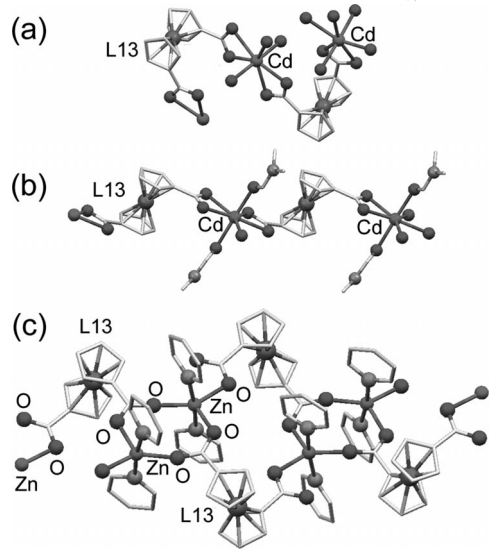


Figure 20. 1D zigzag structures of (a) $[Cd(\mathbf{L13})(H_2O)_3 \cdot 4H_2O]_n$ (**34**), (b) $[Cd(\mathbf{L13})(DMF)_2(H_2O)]_n$ (**35**), and (c) 1D ribbon-like structure of $[Zn_2(\mathbf{L13})_2(pyridine)_4]_n$ (**36**).

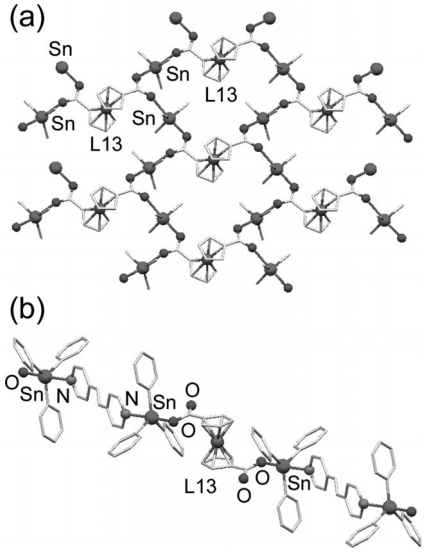


Figure 21. (a) 2D sheet structure of $[(Sn(CH_3)_3)_2(\mathbf{L13})]_n$ (**37**) and (b) 1D chain structure of $[(SnPh_3)_2(\mathbf{L13})(bpe)]_n$ (**40**).

The reaction of $[Cu(tmeda)(NO_3)_2 \cdot H_2O]$ (tmeda = *N*,*N*,*N*′,*N*′-tetramethylethylenediamine) and ferrocenedicarboxylic acid ($\mathbf{L13} \cdot 2H^+$) in the presence of $(nBu_4N)OH$ generates a 1D zigzag chain complex $[Cu(tmeda)(\mathbf{L13})]_n$ (**42**) (Figure 22a).[30] This is in contrast to the corresponding Co and Ni complexes, which form 2:2 M/L discrete macrocyclic structures.[30] A related complex, $[Cu(pmdta)(\mathbf{L13})(H_2O) \cdot$

  

$CH_3OH$] (pmdta = 1,1,4,7,7-*N*,*N*,*N*′,*N*′′,*N*′′-pentamethyldiethylenetriamine), exhibits a discrete structure, in which one of the carboxylate groups in **L13** coordinates to the metal, while the other forms hydrogen bonds with a coordination water of an adjacent unit and a solvate molecule $CH_3OH$ (Figure 22b).[30] The latter carboxylate group acts as a non-coordinating anion.

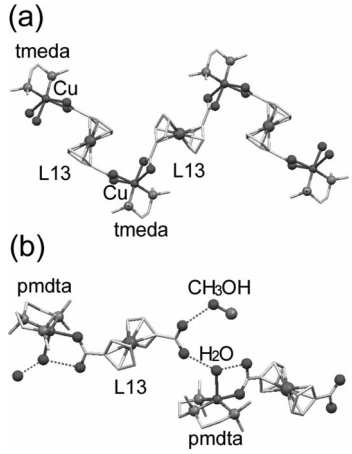


Figure 22. (a) 1D zigzag chain structure of [Cu(tmeda)(**L13**)]$_n$ (**42**) and (b) discrete molecular [Cu(pmdta)(**L13**)($H_2O$)·$CH_3OH$]. Dashed lines in (b) indicate hydrogen bonds.

Through the use of $Ln^{III}$ salts, the dimensionality of the resulting coordination polymers increases because of the high coordination number of the lanthanide ions. [$Y_2$(**L13**)$_3$($H_2O$)$_4$·$H_2O$]$_n$ (**43**) (Figure 23) and related complexes (**44**–**50**) are 2D coordination polymers.[26,31–34] The metal center in **43** is coordinated with nine oxygen atoms from four **L13** ligands and two water molecules. Two **L13** ligands ($\tau$ = 62°) bridge two metal ions to construct a metallamacrocycle, which is further linked by **L13** ($\tau \approx 180°$) to form a 2D brick-wall structure. A weak ferromagnetic interaction (Weiss temperature $\theta$ = 0.93 K) is present between the $Eu^{III}$ ions in **44**.[26]

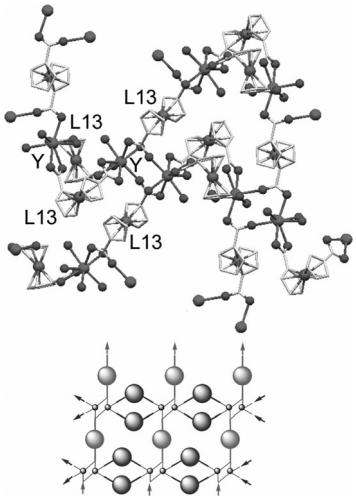


Figure 23. 2D sheet structures of [$Y_2$(**L13**)$_3$($H_2O$)$_4$·$H_2O$]$_n$ (**43**). A schematic illustration of the structure is also shown.

The introduction of additional bridging ligands leads to higher-dimensional structures. [$Cu_2$(**L13**)$_2$(bbim)$_3$·$6H_2O$]$_n$ (**51**) is a 3D coordination polymer (Figure 24a).[35] The assembled structure can be regarded as a pillared layer, with 2D brick walls formed by the $Cu^{II}$ ion and bbim and linked by **L13** ($\tau$ = 131°). The pillared-layer structures are further interpenetrated. The local structure of [Cd(**L13**)(L–L)-($H_2O$)·*m*$H_2O$]$_n$ [L–L = pebbm, *m* = 2 (**52**); L–L = prbbm, *m* = 3 (**53**)] is composed of a macrocycle containing two $Cd^{II}$ ions and two **L13** ligands ($\tau$ = 54° for **52** and 56° for **53**).[36] Despite their similar local structures, the assembled structures of **52** and **53** depend on the additional ligands: **52** has a 1D necklace-like chain structure, while **53** exhibits

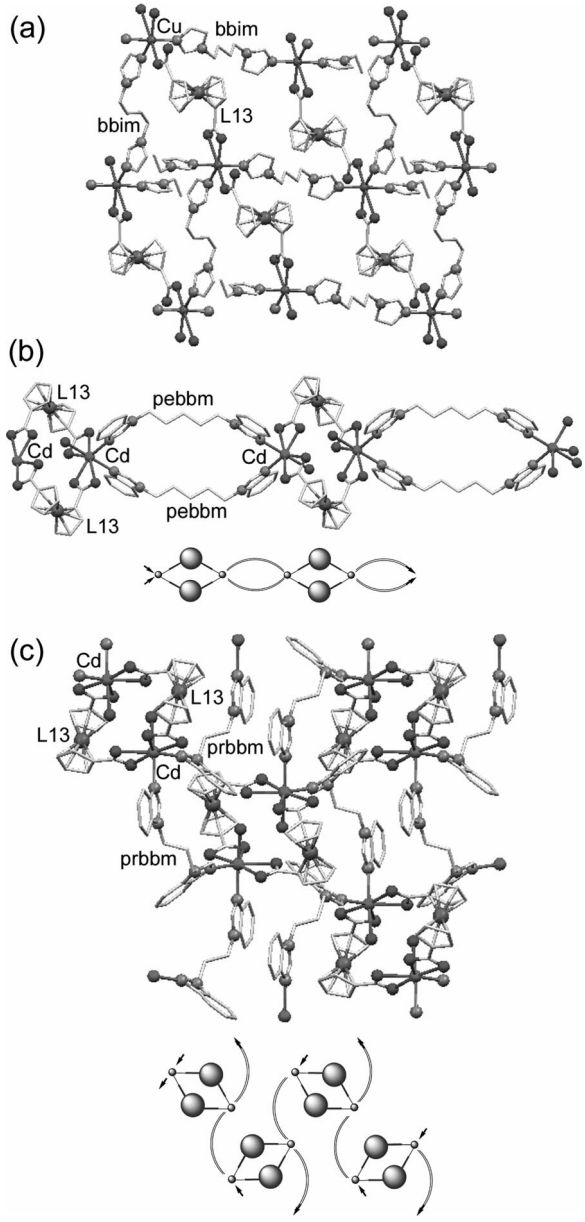


Figure 24. (a) 3D pillared-layer structure of [$Cu_2$(**L13**)$_2$(bbim)$_3$·$6H_2O$]$_n$ (**51**), (b) 1D necklace-like chain structure of [Cd(**L13**)(pebbm)($H_2O$)·$2H_2O$]$_n$ (**52**), and (c) 2D sheet structure of [Cd(**L13**)(prbbm)($H_2O$)·$3H_2O$]$_n$ (**53**). Schematic illustrations of the structures of **52** and **53** are also shown.

  

a 2D sheet structure (Figures 24b and 24c). Several coordination polymers derived from **L13** (**43**, **45**, **46**, **52**, and **53**) show broad luminescence around 390 nm in the solid state, which is assignable to intraligand fluorescent emissions.[26,36]

### Side-Chain Coordination Polymers

Ligands **L14**–**L21** give rise to 1D side-chain coordination polymers, often with complicated coordination structures, similar to complexes containing **L13**. The use of additional bridging ligands leads to chain structures, in which metal-centered clusters with carboxylate ligands are further linked by bridging ligands. The carboxylated ferrocenes in such complexes act mostly as pendants and not as bridging ligands. In this section, we mainly focus on complexes with **L14**, which are typical.

[Sn(*o*-fluorobenzyl)$_3$(**L14**)]$_n$ (**54**) is a simple zigzag 1D side-chain polymer, composed of repeating units of Sn(*o*-fluorobenzyl)$_3$ and **L14** (Figure 25a).[37] This organometallic complex is obtained by the reaction of [SnCl(*o*-fluorobenzyl)$_3$]$_2$ with ferrocenecarboxylic acid (**L14**·H$^+$). Ligand **L14** coordinates to the axial positions of the Sn$^{IV}$ center and links the metal ions with a *syn-anti* bridging mode. [Na$_2$Cd(**L14**)$_4$(CH$_3$OH)$_2$]$_n$ (**55**) (Figure 25b) is a 1D necklace-like chain complex, in which Cd(**L14**)$_4$ units are linked by two Na$^I$ ions.[38] This is an example of a mixed-metal complex. [Pb$_4$(**L14**)$_8$(CH$_3$OH)$_2$·3CH$_3$OH·2H$_2$O]$_n$ (**56**) exhibits a 1D ribbon-like structure, containing alternating units of Pb$_2$O$_2$ and Pb$_2$O$_4$ rhomboids with ferrocenyl pendants (Figure 25c).[39] The complex contains four **L14** ligands with different coordination modes: monodentate, bidentate, tridentate, and tetradentate.[39] As can be seen from the structural variety of these and similar complexes, the assembled structures of complexes with carboxylate ligands are rather unpredictable, in contrast to those with neutral ligands.

The use of *N*-donor bridging ligands together with **L14** leads to 1D polymers, which contrasts with the tendency of **L14** to form 2D structures. The assembled structures of the complexes, as well as their guest inclusion properties, vary depending on the additional ligand. [Zn(**L14**)$_2$(bpp)]$_n$ (**57**) is a zigzag chain complex in which Zn(**L14**)$_2$ is joined by bpp (Figure 26a).[39] The use of bbbm instead of bpp leads to the helical-chain complex [Zn(**L14**)$_2$(bbbm)·2H$_2$O]$_n$ (**58**) (Figure 26b).[40] [Zn$_2$(**L14**)$_4$(bpt)$_2$·5H$_2$O]$_n$ (**59**) is also a 1D

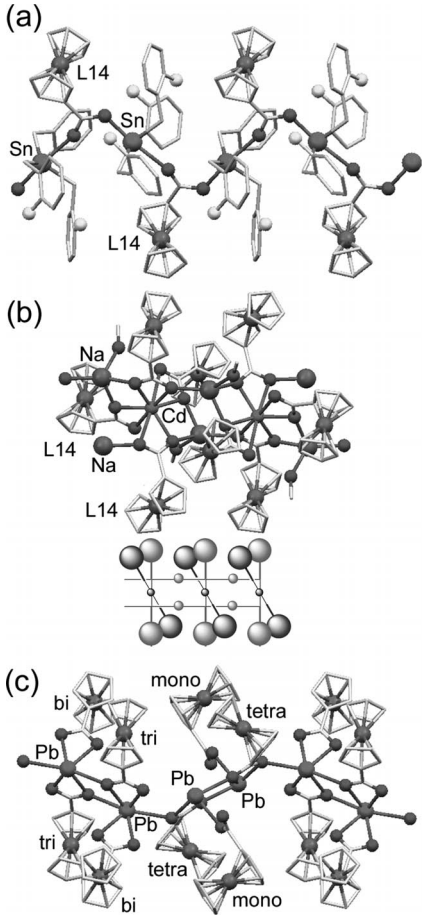


Figure 25. (a) 1D zigzag structure of [Sn(*o*-fluorobenzyl)$_3$(**L14**)]$_n$ (**54**), (b) 1D necklace-like chain structure of [Na$_2$Cd(**L14**)$_4$(CH$_3$OH)$_2$]$_n$ (**55**), and (c) 1D ribbon structure of [Pb$_4$(**L14**)$_8$(CH$_3$OH)$_2$·3CH$_3$OH·2H$_2$O]$_n$ (**56**). A schematic illustration of the structure of **55** is also shown.

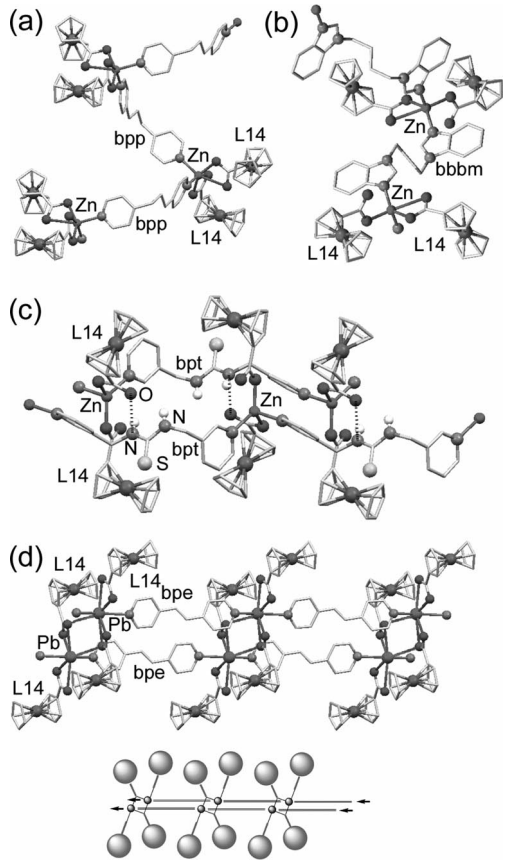


Figure 26. (a) 1D zigzag structure of [Zn(**L14**)$_2$(bpp)]$_n$ (**57**), (b) helical structure of [Zn(**L14**)$_2$(bbbm)·2H$_2$O]$_n$ (**58**), and 1D ladder-like structures of (c) [Zn$_2$(**L14**)$_4$(bpt)$_2$·5H$_2$O]$_n$ (**59**) and (d) [Pb(**L14**)$_2$(bpe)]$_n$ (**60**). A schematic illustration of the structure of **60** is also shown.

  

chain polymer, but due to the presence of the NH group in bpt, two adjacent chains are linked by NH···$O_{ligand}$ hydrogen bonds to form a ladder-like structure (Figure 26c), which is stacked to produce a large porous assembled structure containing guest water molecules.[39] [Pb(**L14**)$_2$(bpe)]$_n$ (**60**) exhibits a ladder-like structure with an alternating arrangement of a [$Pb_2$(**L14**)$_4$] rhomboid and two bpe ligands (Figure 26d).[39]

Ligand **L14** can form lantern-type dinuclear complexes, as is characteristic of carboxylates. A 1D linking of the dinuclear units leads to a side-chain polymer. [{$Mn_2$(**L14**)$_4$}{Mn(**L14**)$_2$($CH_3OH$)$_4$}]$_n$ (**61**) is a 1D coordination polymer (Figure 27) in which lantern-like $Mn_2$ dimer units are bridged by Mn(**L14**)$_2$ units.[41] The addition of bpy to **61** leads to the formation of the 2D sheet complex [{$Mn_2$(**L14**)$_4$}{Mn(**L14**)$_2$(bpy)($H_2O$)$_2$}]$_n$ (**62**), in which the dinuclear unit is highly deformed and the 1D chains are further linked by bpy.[41,42] Complex **61** exhibits an antiferromagnetic interaction ($J \approx -41$ K) between the Mn ions ($S = 5/2$) within the dinuclear unit, while the corresponding interaction in **62** is much smaller ($J \approx -2$ K). The difference is mainly due to the structural difference in the $Mn_2$(**L14**)$_4$ units.[41]

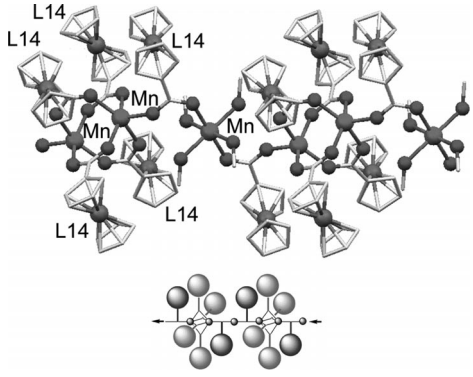


Figure 27. 1D chain structure of [{$Mn_2$(**L14**)$_4$}{Mn(**L14**)$_2$($CH_3OH$)$_4$}]$_n$ (**61**). A schematic illustration of the structure is also shown.

[$UO_2$(**L15**)(THF)·(ferrocene)] (**63**) exhibits a 1D ribbon structure (Figure 28).[43] The $U^{VI}$ center is coordinated with seven oxygen atoms from four carboxylate groups, two oxido groups, and THF. The linear chain consists of an alternating arrangement of a [$UO_2$(THF)] unit and two carboxylate groups from the ligand. The two carboxylate groups of the ligand adopt a *syn-anti* bridging mode and are almost coplanar. The interstices between the linear chains are occupied by free ferrocene. This complex is an unprecedented product of a reaction involving **L14**. Formation of this complex involves the formation of [$UO_2$(**L14**)$_2$], cleavage of the carboxylate group from **L14**, and subsequent formation of **L15** and free ferrocene.

Ligands **L16**–**L20** contain spacer groups between the ferrocenyl moiety and the carboxylate group. In contrast to **L13**, most of the complexes reported involve additional bridging ligands. This tendency may be ascribed to increased flexibility in the ligands. Because the structural

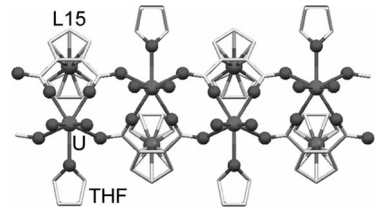


Figure 28. 1D linear chain structure of [$UO_2$(**L15**)(THF)·(ferrocene)] (**63**).

tendencies of such complexes are similar to those of complexes with **L14**, we will limit our discussion to certain interesting complexes. The structure of the 2D sheet complex [$Cd_2$(**L16**)$_4$(bix)$_2$·4$CH_3OH$]$_n$ (**66**) is unique (Figure 29).[45] The local structure around the dimer unit can be regarded as a Möbius-like $Cd_4$(L–L)$_4$ strip surrounding a windmill-like Cd(**L16**)$_4$ unit. Another interesting example is the structural change of 1D polymer [Mn(**L19**)$_2$($\mu^2$-$OH_2$)$_2$($H_2O$)$_2$·$H_2O$]$_n$ (**76**) to a 1D ribbon polymer [Mn(**L19**)$_2$(phen)]$_n$ (**77**) by the addition of phen, along with elimination of the coordinating water molecule (Figure 30).[49] Both $Mn^{II}$ complexes exhibit antiferromagnetic interactions between the $Mn^{II}$ ions (Curie–Weiss temperature $\theta$ = –26.5 K for **76**, –16.0 K for **77**).[49] The assembled structures

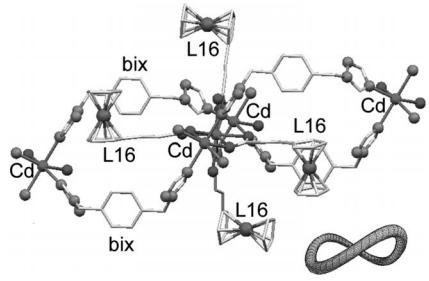


Figure 29. 2D sheet structure of [$Cd_2$(**L16**)$_4$(bix)$_2$·4$CH_3OH$]$_n$ (**66**). A schematic illustration of the structure is also shown.

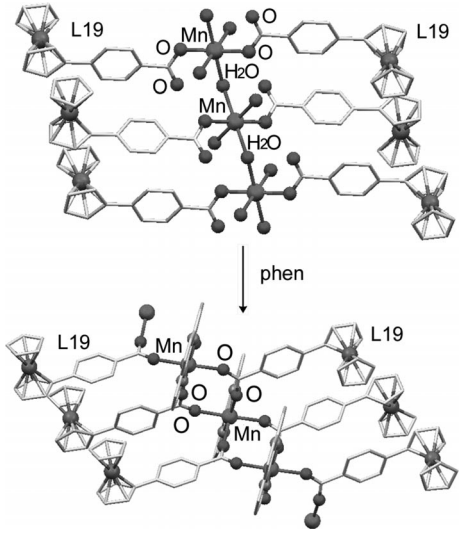


Figure 30. 1D chain structure of [Mn(**L19**)$_2$($\mu^2$-$OH_2$)$_2$($H_2O$)$_2$·$H_2O$]$_n$ (**76**) (top) and 1D ribbon structure of [Mn(**L19**)$_2$(phen)]$_n$ (**77**) (bottom).

  

and guest inclusion properties of $[M(\mathbf{L20})_2(L–L)(sol.)_2 \cdot 2(guest)]_n$ (M = Cd, Zn, Pb; L–L = bpe, bpy, pebbm; sol. or guest = $CH_3OH$, $H_2O$) (**81**–**84**), which depend on the shape of the additional ligand, are notable.[46,50] Several complexes with ferrocene carboxylate derivatives show nonlinear optical refraction effects with self-focusing behavior.[44,48]

The structurally related β-diketonate ligand **L21** affords the linear chain complex $[Zn(\mathbf{L21})_2(bpe)]_n$ (**85**) by addition of a secondary ligand (Figure 31).[51] In this complex, $Zn^{II}$ ions chelated by **L21** are further linked by bpe. This example demonstrates a useful method of preparing side-chain coordination polymers by using chelating ligands.

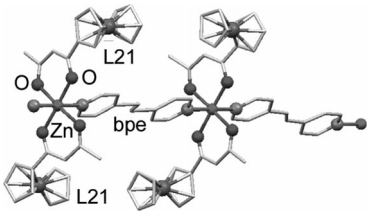


Figure 31. 1D linear structure of $[Zn(\mathbf{L21})_2(bpe)]_n$ (**85**).

## Coordination Polymers from Sulfonated Ferrocenes

Ligand **L22** affords high-dimensional main-chain coordination polymers in combination with *N*-donor bidentate ligands, for which characteristic properties such as gas adsorption and ion exchange have been demonstrated. $[Cd(\mathbf{L22})(bpp)_2 \cdot 2CH_3OH \cdot 6H_2O]_n$ (**86**) is a 2D sheet complex, in which rhomboids composed of $Cd^{II}$ ions and two bpp molecules are bridged by antiperiplanar **L22** ($\tau \approx 180°$) (Figure 32a).[52] The 2D layers are stacked, and the structure contains large cavities. $[Cd(\mathbf{L22})(bpy)_2 \cdot 4CH_3OH]_n$ (**87**) possesses an interpenetrated pillared-layer structure composed of 2D sheets of $Cd^{II}$ and two bpy molecules, which are linked by **L22** ($\tau \approx 180°$) (Figure 32b).[52] Both **86** and **87** show marked gas absorption properties due to their porous structures. In addition, **87** undergoes unique ion exchange reactions when immersed in aqueous solutions containing divalent metal ions, while maintaining its single-crystal state. The rate of exchange depends on the metal ion and the counteranion.

Complexation of **L23** with $Zn^{II}$ in the presence of bpy produces a pillared-layer 2D complex $[Zn(\mathbf{L23})_2(bpy)_2]_n$ (**88**) with a side-chain structure.[53] This complex exhibits a 2D sheet structure in which the $Zn^{II}$ ion and two bpy molecules form a 2D lattice with **L23** ligands located above and below the sheet (Figure 33). This complex participates in ion exchange reactions, as observed in complexes with **L22** (**86** and **87**). When single crystals of **88** are impregnated with a methanol solution of $M(NO_3)_2$ (M = Cd, Pb, and Cu), an ion exchange reaction takes place to produce single crystals of $[Zn_{1-x}M_x(\mathbf{L23})_2(bpy)_2]_n$.[53]

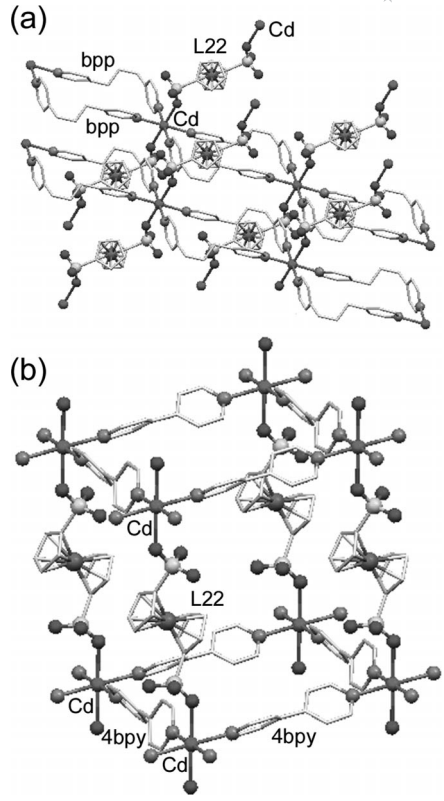


Figure 32. (a) 2D sheet structure of $[Cd(\mathbf{L22})(bpp)_2 \cdot 2CH_3OH \cdot 6H_2O]_n$ (**86**) and (b) 3D pillared-layer structure of $[Cd(\mathbf{L22})(bpy)_2 \cdot 4CH_3OH]_n$ (**87**).

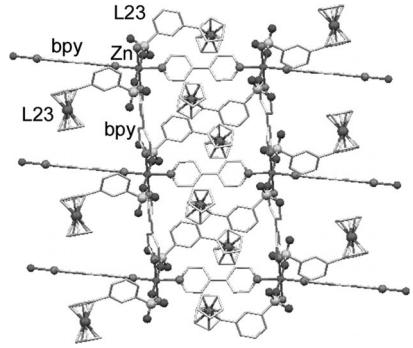


Figure 33. 2D sheet structure of $[Zn(\mathbf{L23})_2(bpy)_2]_n$ (**88**).

## Coordination Polymers from Unsymmetrical Ferrocenes

**L24** and **L25** are probably the only examples of 1,1′-disubstituted unsymmetrical ferrocene ligands that afford main-chain coordination polymers, and to the best our knowledge, there are no side-chain coordination polymers with unsymmetrical ferrocene ligands. Ligand **L24** produces 1D coordination polymers $[MBr_2(\mathbf{L24})]_n$ [M = Cd (**89**; Figure 34a), Hg], in which both the P and N atoms of the ligand coordinate to the metal ions.[55a] The ferrocene moiety in **89** adopts an anticlinal conformation ($\tau$ = 157°). The presence of "hard" and "soft" donor atoms in the ligand is particularly interesting. When metal complexation is carried

  

out under acidic conditions, a discrete metal complex is produced, in which the P donor atom coordinates to the metal ion, while the N atom is protonated.[55a] The combination of **L25** and $CdBr_2$ produces a 1D coordination polymer $[(CdBr_2)_2(\mathbf{L25})_2]_n$ (**90**) (Figure 34b), in which **L25** acts as an $O^1$, $P^2$-bridging ligand. In the structure, macrocycles, constructed of two anticlinal **L25** ligands and two $Cd^{II}$ ions, are linked by a halogen bridge.[55b] This is in contrast with related $Zn^{II}$ and $Hg^{II}$ complexes, which show 1:1 and 2:2 M/L discrete structures, respectively.[55b] The structure of the $Hg^{II}$ complex closely resembles the local structure of **90**.

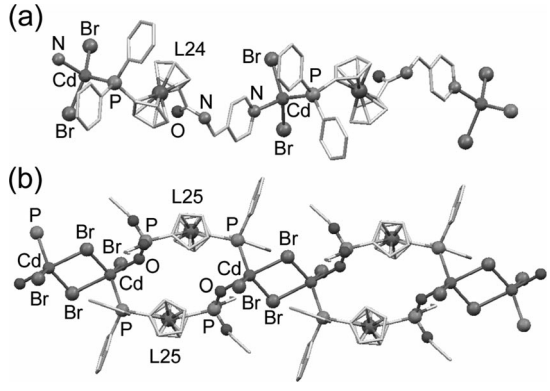


Figure 34. 1D structures of (a) $[CdBr_2(\mathbf{L24})]_n$ (**89**) and (b) $[(CdBr_2)_2(\mathbf{L25})_2]_n$ (**90**).

## Summary and Perspectives

This review has illustrated that main-chain and side-chain ferrocene-containing polymers can be synthesized on the basis of rational ligand design. These polymers exhibit a structural diversity that is based on conformational flexibility and various coordination modes of the ferrocene-based ligands. The structures are mostly one-dimensional, but characteristic structural changes result from the use of additional bridging ligands in complexes with anionic ligands. These studies may be extended to other metallocene systems, and the strategy can also be applied to other metal-containing ligands.

As described above, coordination polymers derived from ferrocene-based ligands show characteristic physical properties, such as redox, magnetism, luminescence, nonlinear optical properties, and ion-exchange. These properties, however, are not unprecedented in coordination polymers, and exploring unique properties characteristic to ferrocene or metallocene coordination polymers is of significant interest. From this viewpoint, unsymmetrical ferrocene ligands carrying different donor moieties are interesting with regard to their potential to generate chemically and physically interesting heteronuclear and hemilabile complexes. The development of porous metallocene-containing coordination polymers is also an interesting research target, and various functions such as catalytic activity, multistep redox activity, and magnetic properties may be realized. Additionally, magnetic coordination polymers containing metallocenium cations, which are interesting from the viewpoint of molecular magnetism, have yet to be developed. The studies discussed in this review are also useful as a foundation for the construction and analysis of functional 2D assemblies on surfaces.

## Acknowledgments

This work was supported by a Grant-in-Aid for Scientific Research (No. 21350077) from the Japan Society for the Promotion of Science (JSPS). We thank Mr. T. Inagaki and Mr. A. Funabiki (Kobe University) for their help with literature searches. R. H. wishes to express his thanks to Mr. B. Kessler (Johnson Matthey Japan, Inc.) and Dr. N. Ishihara (Idemitsu Kosan Co., Ltd.) for their continued encouragement. We also thank the anonymous reviewers for their valuable comments.

[1] a) *Chem. Soc. Rev.* **2009**, *38*, 1201–1508 (themed issue "Metal–Organic Frameworks" and references cited therein); b) Z. Wang, G. Chen, K. Ding, *Chem. Rev.* **2009**, *109*, 322–359; c) R. Horikoshi, T. Mochida, *Coord. Chem. Rev.* **2006**, *250*, 2595–2609; d) *Coord. Chem. Rev.* **2003**, *246* (Special issue on structure, properties and application of inorganic polymers, and references cited therein); e) C. Janiak, *Dalton Trans.* **2003**, 2781–2804; f) S. R. Batten, S. M. Neville, D. R. Turner, *Coordination Polymers: Design, Analysis and Application*, RSC Publishing, London, **2009**; g) D. Braga, F. Grepioni, A. G. Orpen (Eds.), *Crystal Engineering, From Molecules and Crystals to Materials*, Kluwer Academic Publishers, The Netherlands, **1999**; h) J.-M. Lehn, *Supramolecular Chemistry, Concepts and Perspectives*, Wiley-VCH, Weinheim, **1995**.

[2] a) P. Štěpnička (Ed.), *Ferrocenes: Ligands, Materials and Biomolecules*, John Wiley & Sons. Ltd., Chichester, **2008**; b) *J. Organomet. Chem.* **2001**, *637–639* (Special issue, 50th Anniversary of the Discovery of Ferrocene, and references cited therein); c) G. Bandoli, A. Dolmella, *Coord. Chem. Rev.* **2000**, *209*, 161–196; d) A. Togni, T. Hayashi (Eds.), *Ferrocenes: Homogenous Catalysis, Organic Synthesis Materials Science*, Wiley-VCH, Weinheim, **1995**.

[3] a) M. J. MacLachlan in *Frontiers in Transition-Metal-Containing Polymers* (Eds.: A. S. A.-E.-Aziz, I. Manners), John Wiley & Sons, Hoboken, **2007**, pp. 161–216; b) U. S. Schubert, G. R. Newkome, I. Manners (Eds.), *Metal-Containing and Metallosupramolecular Polymers and Materials*, ACS Symposium Series, **2006**, vol. 928; c) P. Nguyen, P. Gómez-Elipe, I. Manners, *Chem. Rev.* **1999**, *99*, 1515–1548; d) C. E. Carraher Jr., J. E. Sheats, C. U. Pittman Jr., (Eds.), *Organometallic Polymers*, Academic Press, Inc., New York, **1978**; e) E. J. Becker, M. Tsutsui (Eds.), *Organometallic Reactions and Syntheses*, Plenum Press, New York, **1977**; f) C. U. Pittman Jr., *J. Polym. Sci. A-1* **1968**, *6*, 1687–1695; g) J. C. Lai, T. Rounsfell, C. U. Pittman, *J. Polym. Sci. A-1* **1971**, *9*, 651–662.

[4] a) R. Horikoshi, T. Mochida, H. Moriyama, *Inorg. Chem.* **2002**, *41*, 3017–3024; b) R. Horikoshi, M. Ueda, T. Mochida, *New J. Chem.* **2003**, *27*, 933–937.

[5] a) R. Horikoshi, C. Nambu, T. Mochida, *Inorg. Chem.* **2003**, *42*, 6868–6875; b) R. Horikoshi, K. Okazawa, T. Mochida, *J. Organomet. Chem.* **2005**, *690*, 1793–1799; c) T. Mochida, H. Shimizu, K. Okazawa, *Inorg. Chim. Acta* **2007**, *360*, 2175–2180.

[6] L.-T. Phang, T. S. A. Hor, Z.-Y. Zhou, T. C. W. Mak, *J. Organomet. Chem.* **1994**, *469*, 253–261.

[7] A. Houlton, D. M. P. Mingos, D. M. Murphy, D. J. Williams, L.-T. Phang, T. S. A. Hor, *J. Chem. Soc., Dalton Trans.* **1993**, 3629–3630.

[8] D. T. Hill, G. R. Girard, F. L. McCabe, R. K. Johnson, P. D. Stupik, J. H. Zhang, W. M. Reiff, D. S. Eggleston, *Inorg. Chem.* **1989**, *28*, 3529–3533.

  

[9] a) X. L. Lu, W. K. Leong, L. Y. Goh, A. T. S. Hor, *Eur. J. Inorg. Chem.* **2004**, 2504–2513; b) C. D. Nicola, Effendy, C. Pettinari, B. W. Skelton, N. Somers, A. H. White, *Inorg. Chim. Acta* **2005**, *358*, 695–706.
[10] D. R. Smyth, J. Hester, V. G. Young Jr., E. R. T. Tiekink, *CrystEngComm* **2002**, *4*, 517–521.
[11] M. C. Gimeno, P. G. Jones, A. Laguna, C. Sarroca, *J. Chem. Soc., Dalton Trans.* **1998**, 1277–1280.
[12] T. Avilés, A. Dinis, J. O. Gonçalves, V. Félix, M. J. Calhorda, Â. Prazeres, M. G. B. Drew, H. Alves, R. T. Henriques, V. da Gama, P. Zanello, M. Fontani, *J. Chem. Soc., Dalton Trans.* **2002**, 4545–4602.
[13] T. Weidner, N. Ballav, M. Zharnikov, A. Priebe, N. J. Long, J. Maurer, R. Winter, A. Rothenberger, D. Fenske, D. Rother, C. Bruhn, H. Fink, U. Siemeling, *Chem. Eur. J.* **2008**, *14*, 4346–4360.
[14] E. M. Barranco, O. Crespo, M. C. Gimeno, P. G. Jones, A. Laguna, C. Sarroca, *J. Chem. Soc., Dalton Trans.* **2001**, 2523–2529.
[15] O. Crespo, M. C. Gimeno, P. G. Jones, A. Laguna, C. Sarroca, *Chem. Commun.* **1998**, 1481–1482.
[16] S. Canales, O. Crespo, A. Fortea, M. C. Gimeno, P. G. Jones, A. Laguna, *J. Chem. Soc., Dalton Trans.* **2002**, 2250–2255.
[17] a) E. M. Barranco, O. Crespo, M. C. Gimeno, P. G. Jones, A. Laguna, M. D. Villacampa, *J. Organomet. Chem.* **1999**, *592*, 258–264; b) O. Carugo, G. De Santis, L. Fabbrizzi, M. Licchelli, A. Monichino, P. Pallavicini, *Inorg. Chem.* **1992**, *31*, 765–769.
[18] a) J. G. P. Delis, P. W. N. M. van Leeuwen, K. Vrieze, N. Veldman, A. L. Spek, J. Fraanje, K. Goubitz, *J. Organomet. Chem.* **1996**, *514*, 125–136; b) K. Tani, T. Mihana, T. Yamagata, T. Saito, *Chem. Lett.* **1991**, 2047–2050; c) D. Braga, M. Polito, M. Bracaccini, D. D'Addario, E. Tagliavini, D. M. Proserpio, F. Grepioni, *Chem. Commun.* **2002**, 1080–1081.
[19] T. Mochida, K. Okazawa, R. Horikoshi, *Dalton Trans.* **2006**, 693–704.
[20] a) M. Li, P. Cai, C. Duan, F. Lu, J. Xie, Q. Meng, *Inorg. Chem.* **2004**, *43*, 5174–5176; b) A. Ion, M. Buda, J.-C. Moutet, E. Saint-Aman, G. Royal, I. Gautier-Luneau, M. Bonin, R. Ziessel, *Eur. J. Inorg. Chem.* **2002**, 1357–1366; c) A. Ion, J.-C. Moutet, E. Saint-Aman, G. Royal, S. Tingry, J. Pecaut, S. Menage, R. Ziessel, *Inorg. Chem.* **2001**, *40*, 3632–3636; d) J. D. Carr, S. J. Coles, M. B. Hursthouse, H. R. Tucker, *J. Organomet. Chem.* **2001**, *637–639*, 304–310.
[21] C.-Y. Cao, K.-J. Wei, J. Ni, Y. Liu, *Inorg. Chem. Commun.* **2010**, *13*, 19–21.
[22] a) K.-J. Wei, J. Ni, Y. Liu, *Inorg. Chem.* **2010**, *49*, 1834–1848; b) K.-J. Wei, J. Ni, Y.-S. Xie, Y. Liu, Q.-L. Liu, *Dalton Trans.* **2007**, 3390–3397.
[23] C.-j. Fang, C.-y. Duan, D. Guo, C. He, Q.-j. Meng, Z.-m. Wang, C.-h. Yan, *Chem. Commun.* **2001**, 2540–2541.
[24] D. L. Reger, K. J. Brown, J. R. Gardinier, M. D. Smith, *Organometallics* **2003**, *22*, 4973–4983.
[25] a) A. L. Gavrilova, B. Bosnich, *Chem. Rev.* **2004**, *104*, 349–384; b) M. Casarin, C. Corvaja, C. Di Nicola, D. Falcomer, L. Franco, M. Monari, L. Pandolfo, C. Pettinari, F. Piccinelli, *Inorg. Chem.* **2005**, *44*, 6265–6276.
[26] X. Meng, G. Li, H. Hou, H. Han, Y. Fan, Y. Zhu, C. Du, *J. Organomet. Chem.* **2003**, *679*, 153–161.
[27] D. Guo, H. Mo, C.-Y. Duan, F. Lu, Q.-J. Meng, *J. Chem. Soc., Dalton Trans.* **2002**, 2593–2594.
[28] S.-W. Leng, G. Wu, M.-H. Xin, L.-L. Tang, G.-S. Zhu, Y. Fan, S.-H. Shi, *Chem. J. Chin. Univ.* **2004**, *25*, 817–819.
[29] V. Chandrasekhar, R. Thirumoorthi, *Dalton Trans.* **2010**, *39*, 2684–2691.
[30] J. Kühnert, T. Rüffer, P. Ecorchard, B. Bräuer, Y. Lan, A. K. Powell, H. Lang, *Dalton Trans.* **2009**, 4499–4508.
[31] D. Guo, Y. T. Li, C. Y. Duan, H. Mo, Q. J. Meng, *Inorg. Chem.* **2003**, *42*, 2519–2530.
[32] Y.-Y. Yang, W.-T. Wong, *Chem. Commun.* **2002**, 2716–2717.
[33] D. Guo, B. G. Zhang, C. Y. Duan, X. Cao, Q. J. Meng, *Dalton Trans.* **2003**, 282–284.
[34] L.-L. Meng, B.-G. Zhang, Z.-H. Peng, J.-G. Ren, P. Cai, C.-Y. Duan, *Chin. J. Inorg. Chem.* **2004**, *20*, 1228–1232.
[35] J. Yang, J.-F. Ma, Y.-Y. Liu, S.-L. Li, G.-L. Zheng, *Eur. J. Inorg. Chem.* **2005**, 2174–2180.
[36] L. Wang, X. Meng, E. Zhang, H. Hou, Y. Fan, *J. Organomet. Chem.* **2007**, *692*, 4367–4376.
[37] D.-Z. Kuang, Z.-M. Chen, F.-X. Zhang, J.-Q. Wang, Y.-L. Feng, *Chin. J. Inorg. Chem.* **2006**, *22*, 1947–1951.
[38] S.-J. Zhou, M.-S. Chen, Z.-L. Chen, F.-P. Liang, L.-L. Wei, *Chin. J. Inorg. Chem.* **2005**, *21*, 1791–1797.
[39] H. Hou, L. Li, G. Li, Y. Fan, Y. Zhu, *Inorg. Chem.* **2003**, *42*, 3501–3508.
[40] G. Li, Z. Li, H. Hou, X. Meng, Y. Fan, W. Chen, *J. Mol. Struct.* **2004**, *694*, 179–183.
[41] Z. Chen, Y. Ma, F. Liang, Z. Zhou, *Eur. J. Inorg. Chem.* **2007**, 2040–2045.
[42] W.-J. Lu, Y.-M. Zhu, K.-L. Zhong, *Acta Crystallogr., Sect. C Cryst. Struct. Commun.* **2007**, *63*, m4–m6.
[43] A. E. Vaughn, C. L. Barnes, P. B. Duval, *Angew. Chem. Int. Ed.* **2007**, *46*, 6622–6625.
[44] L. K. Li, Y. L. Song, H. W. Hou, Y. T. Fan, Y. Zhu, *Eur. J. Inorg. Chem.* **2005**, 3238–3249.
[45] X. Wang, L. Li, H. Hou, J. Wu, Y. Fan, *Eur. J. Inorg. Chem.* **2007**, 5234–5245.
[46] G. Li, H. Hou, L. Li, X. Meng, Y. Fan, Y. Zhu, *Inorg. Chem.* **2003**, *42*, 4995–5004.
[47] G. Li, H. Hou, Z. Li, X. Meng, Y. Fan, *New J. Chem.* **2004**, *28*, 1595–1599.
[48] J. Li, Y. Song, H. Hou, M. Tang, Y. Fan, Y. Zhu, *J. Organomet. Chem.* **2007**, *692*, 1584–1592.
[49] H. Hou, L. Li, Y. Zhu, Y. Fan, Y. Qiao, *Inorg. Chem.* **2004**, *43*, 4767–4774.
[50] G. Li, Z.-F. Li, J.-X. Wu, C. Yue, H.-W. Hou, *J. Coord. Chem.* **2008**, *61*, 464–471.
[51] G. Li, H. Hou, Y. Zhu, X. Meng, L. Mi, Y. Fan, *Inorg. Chem. Commun.* **2002**, *5*, 929–932.
[52] L. Mi, H. Hou, Z. Song, H. Han, H. Xu, Y. Fan, S.-W. Ng, *Cryst. Growth Des.* **2007**, *7*, 2553–2561.
[53] L. Mi, H. Hou, Z. Song, H. Han, Y. Fan, *Chem. Eur. J.* **2008**, *14*, 1814–1821.
[54] a) R. G. Arrayás, J. Adrio, J. C. Carretero, *Angew. Chem. Int. Ed.* **2006**, *45*, 7674–7715; b) R. C. J. Atkinson, V. C. Gibson, N. J. Long, *Chem. Soc. Rev.* **2004**, *33*, 313–328.
[55] a) P. Štěpnička, I. Císařová, R. Gyepes, *Eur. J. Inorg. Chem.* **2006**, 926–938; b) J. Kühnert, I. Císařová, M. Lamač, P. Štěpnička, *Dalton Trans.* **2008**, 2454–2464.
[56] a) R. Horikoshi, C. Nambu, T. Mochida, *New J. Chem.* **2004**, *28*, 26–33; b) D. Braga, M. Polito, M. Bracaccini, D. D'Addario, E. Tagliavini, L. Sturba, *Organometallics* **2003**, *22*, 2142–2150.
[57] a) J.-P. Zhang, X.-C. Huang, X.-M. Chen, *Chem. Soc. Rev.* **2009**, *38*, 2385–2396; b) B. Moulton, M. J. Zaworotko, *Chem. Rev.* **2001**, *101*, 1629–1658; c) M. J. Zaworotko, *Chem. Commun.* **2001**, 1–9.
[58] U. Siemeling, A. Girod, D. Rother, C. Bruhn, *Z. Anorg. Allg. Chem.* **2009**, *635*, 1402–1406.
[59] a) T. Ezuhara, K. Endo, K. Matsuda, Y. Aoyama, *New J. Chem.* **2000**, *24*, 609–613; b) F. Lloret, G. De Munno, M. Julve, J. Cano, R. Ruiz, A. Caneschi, *Angew. Chem. Int. Ed.* **1998**, *37*, 135–138.

Received: May 12, 2010
Published Online: October 28, 2010

  